J. Membrane Biol. 103, 95–120 (1988)

The Journal of
Membrane Biology

Topical Review

Structural Basis for E_1–E_2 Conformational Transitions in Na,K-Pump and Ca-Pump Proteins

Peter Leth Jørgensen and Jens Peter Andersen
Danish Biotechnology Research Center for Membrane Proteins, Institute of Physiology, Aarhus University, 8000 Aarhus C, Demark

I. Introduction

The primary active transport of Na^+, K^+, Ca^{2+} and H^+ in eukaryotic cells is driven by ATP-powered cation pumps, the Na,K pump, Ca pump and H,K pump. The intermediary steps of the pump reactions and their relationship to cation translocation have been examined in detail, particularly for the Na,K-pump and Ca-pump proteins. A common feature of these pumps is a protein of M_r close to 110,000 that binds ATP and accepts its γ-phosphate in a covalent Asp-P bond. There is evidence that both phospho- and dephospho-forms of the protein exist in two major conformational states, E_1 and E_2, with different affinities and orientation of cation binding sites, and ATP-driven cation pumping is blocked by micromolar concentrations of vanadate [39, 68, 95, 96, 116, 132]. A wealth of structural information about the cation pump proteins appeared recently after identification of mRNA and sequencing of cloned cDNA. Several isoforms of the genes of α-subunit of Na,K pump were identified in the human and rat genomes [147, 182] and the sequences of α-subunit [110, 111, 145, 146, 178, 181] and β-subunit [22, 112, 140, 146, 179] were deduced from cDNA of mRNA from a variety of tissues in piscine and mammalian species. A similar intensity of work in adjacent fields provided the sequences of slow and fast twitch Ca pump from sarcoplasmic reticulum [19, 121] and H,K pump from stomach mucosa [180]. In addition the gene sequences are available for K pumps [82, 185] and H pumps [1, 177] from microorganisms. As paradigm for interpretation of this information the combined X-ray crystallographic structure at high resolution and amino acid sequences are only available for a few bacterial membrane proteins [38, 129]. Crystals of the proteins of membrane bound Na,K pump [79]. Ca pump [49] and H,K pump [159] can be prepared by incubation in vanadate solution, but only low resolution (>20–25 Å), three-dimensional models can be constructed on this basis.

In this review we will examine basic problems related to the molecular mechanism of active cation transport in light of the information about nucleotide and amino acid sequences. A main purpose is to assign residues involved in formation of ligand binding sites and in E_1–E_2 transition to their position in the sequence. To explain mechanisms of transduction of scalar energy in ATP to movement of cations, it is important to characterize the relationship of conformational changes to translocation of cations across the membrane and the organization of cation pathways. Another problem that must be resolved before meaningful molecular models can be constructed is the question of subunit structure. Recent progress in the characterization of soluble Na,K-ATPase, Ca-ATPase, and H-ATPase suggests that protomer units provide the structural basis for formation of cation pathways [3, 71, 98, 202, 203].

II. Evolution of Cation Pump Proteins

A comparison of Na,K, H,K, Ca, H and K pumps shows that overall sequence homology is moderate, 17–24% except for 63% between H,K-ATPase and Na,K-ATPase, while tertiary structure is remarkably similar with respect to localization of transmembrane segments relative to domains involved in ATP binding and phosphorylation (Fig. 1). The homologies are most pronounced in segments connecting transmembrane helices (M4 and M5) with

Key Words Na,K-ATPase · Ca-ATPase · E_1–E_2-transitions · proteolytic cleavage · active cation transport mechanism

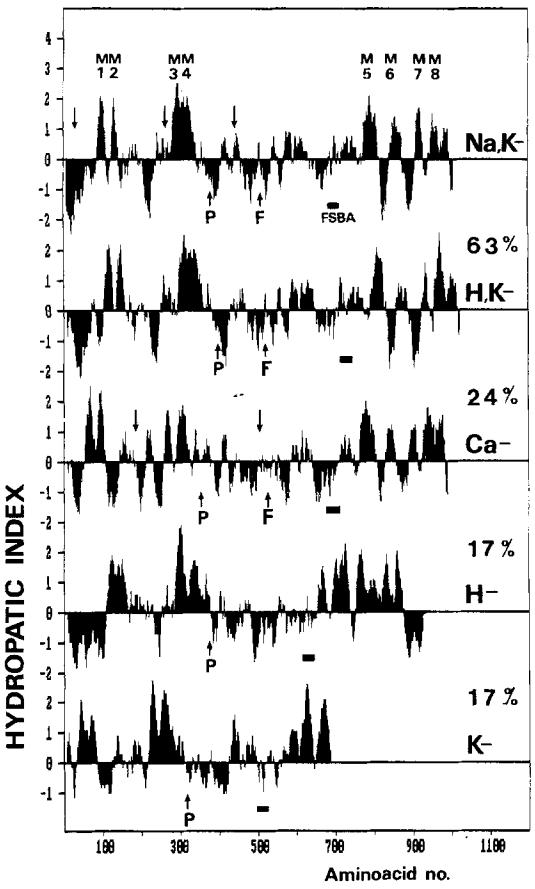

Fig. 1. Hydroplots using a window of 19 residues [117] of Na,K- [111], H,K- [180], Ca- [19], H- [177], and K- [82] pump proteins with percent overall homology (%) in alignment with α-subunit of Na,K-ATPase shown to the right. *M1–M8* show positions of presumptive transmembrane helices. *P* is the phosphorylated residue, *F* the position for covalent insertion of FITC [104], ■ marks the segment labeled with FSBA [33, 141]. The sequences of these segments are shown in Table 1. Vertical arrows mark the positions of primary tryptic cleavage sites. Computer analysis using "Genepro," Riverside Scientific, Seattle, Washington, with the help of Dr. T.E. Petersen

the phosphorylation site and the nucleotide binding area, respectively, while there is little or no homology between the amino acid sequences of N-termini, transmembrane helices, and presumptive cation binding areas in Na,K-ATPase, Ca-ATPase, H-ATPase, and K-ATPase.

Homologies between cation pumps and other ATP binding proteins that are discussed in Section VII, suggest that they have a common origin as shown in Fig. 2 [*cf.* 199]. The molecular basis for evolution of the family of cation pumps from a common ancestor may be gene duplication and drift or fusion and splicing of the gene sequences [42, 67]. Comparison of sequences in Figs. 1 and 3 show that divergence of cation pump genes may have preceeded by recombination of exons involved in recognition, binding of cation and formation of transcellular pathways, in accordance with the needs for cation specificity. Exons coding for domains involved in nucleotide binding, phosphorylation and energy transduction are ancient and the best conserved.

The evolutionary tree in Fig. 2 is drawn on basis of the information in nucleotide and deduced amino acid sequences. K-ATPase of *Streptococcus faecalis* [185] is the most simple and primitive form of cation pump that may represent an ancestral form, but the properties of the protoorganism existing 3–4 billion years ago [37, 123] are not known. The time span of evolution of isoforms of α-subunit of Na,K-ATPase and Ca-ATPase is estimated from mutation rates obtained from comparison of sequences from various species and the time of divergence of phyletic lines [42, 147]. It is seen from Fig. 3 that the mutation rates vary considerably among exons within each gene. Average mutation rates of α-subunit are relatively low, 0.4 per residue per 10^9 years, as compared to rates of 1–2 per residue per 10^9 years for other proteins [147]. Divergence of α, $\alpha+$, and α-III isoforms of Na,K-ATPase may thus have occurred about 300 million years ago at the time of separation of mammalian from piscine lines. Both the cation pumps and ($\Delta\mu$Na)-driven secondary active cotransport systems in eukaryotic cells as alternative to ($\Delta\mu H^+$)-driven systems may have evolved before division of prokaryotes and eukaryotes occurred [184]. Development of Na and Ca pumps and secondary active transport systems for nutrients may form the basis for adaptation to changes in food supply and appearance of a variety of new animal species during transition from precambrian to cambrian period, 700 to 500 million years ago [123].

III. Cation Pump Genes

A. Genes of Na,K-ATPase

The first impression of the genes of the Na,K pump is one of diversity and complexity with at least five genes of α-subunit isoforms with sizes near 20–25 kb. They have multiple introns, comprising more than 80% of known gene sequences. [147, 182]. At least three mRNA isoforms of α-subunit are expressed in rat brain [81, 178]. Clarification of DNA structure and mechanisms behind expression of isoforms is important for understanding organization of the protein in the membrane and physiological pump functions. The positions of the introns may correspond to functional subdivision of the protein

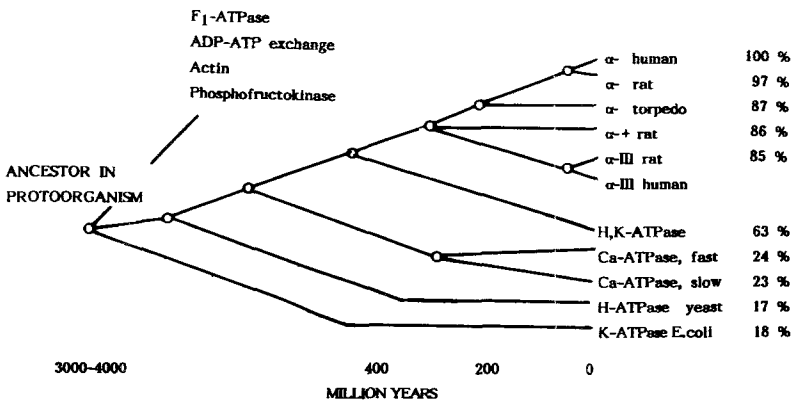

Fig. 2. Evolutionary tree for cation-pump proteins with overall homologies relative to α-subunit of Na,K-ATPase shown to the right. Sequence homologies and references are shown in Table 1. Time scales are based on information about divergence of phyletic lines [37]

[67, 150], in particular to the position of presumed membrane-spanning helices [115].

Chromosome mapping shows that the α-subunit gene is located on human chromosome 1p and on chromosome 3 in mouse. In situ mRNA hybridization shows that α isoform is expressed in transport epithelia particularly in kidney and in cranial and dorsal root ganglia. The α+ gene is localized in human chromosome 1q and α+ is expressed in brain and adult heart ventricle. The α-III gene is found in human chromosome 19q and α-III is expressed in high levels in brain, spinal cord and fetal heart [171]. Screening of human genomic libraries with α-subunit [^{32}P]-cDNA so far revealed five genes. Two were identified in a library from human placenta [147], one related to the α isoform, the other to the α-III isoform. In a genomic library from human leukocytes four genes αA, αB, αC and αD were identified by restriction mapping. Using isoform-specific probes it was shown that αA and αB encode α and α+ isoforms, respectively. The two remaining genes αC and αD do not correspond to previously identified isoforms and it is not known if they are expressed [182].

Partial sequencing of the α-III gene shows that it is a large, 20–25 kb, and complex structure with 22 introns separating the exons (Fig. 3). In contrast, only four introns are found in the gene of H-ATPase in *Neurospora crassa* [1] and the gene of H-ATPase in yeast has no introns [177].

Examination of intron-exon boundaries in the sequence of α-III gene shows that most introns start with GT and end with a stretch of pyrimidines (CT) followed by AG; but assignment of several intron boundaries is uncertain if the AGGT consensus sequence is used as criterion [150]. Search for consensus sequences in the corresponding positions of cDNA for α-subunit from human HeLa cells [111] identified in positions corresponding to amino acid residues 206 (AGGT), 244 (AGGC), 606 (AGGT), and 758 (AGGT). These introns separate exons coding for domains that are among the best preserved when the deduced amino acid sequences of the three α-isoform are compared with those of H,K-ATPase [180] or Ca-ATPase [19].

These and other intron positions correspond to boundaries between functional domains of the α-subunit as shown in Fig. 3. Thus, several transmembrane segments (M1, M2, M3, M6, M7, and M8) are bordered by introns, like in the murine gene of capnophorin [115]. Similarly, introns separate exons corresponding to domains contributing to the different components of the area for nucleotide binding (exons 11, 15, and 16) or phosphorylation (exon 9) that are among the best conserved. Thus, exons 13 and 16 code for segments with close to 100% amino acid homology between the isoforms and higher than average homology with H,K-ATPase and Ca-ATPase. Other exons (nos. 1–3, 10, 19) relate to domains in which homologies between α-isoforms are well below overall homology (89%). Calculation of relative homologies within exons is of interest for identifying specific functional regions. For example, in exons 7 and 17, α-isoforms show homology mutually and with H,K-ATPase, but not with Ca-ATPase suggesting that segments contributing to K sites may be located here. Exons 20 and 21 may correspond to domains that are specific for the Na,K pump, such as Na sites, the ouabain site, or areas for interaction with β-subunit, since there is high mutual homology between α isoforms, while homology with H,K-ATPase and Ca-ATPase is well below the average value. This illustrates that localization of intron positions in genomic DNA will be important for understanding functional subdivision of α-subunit.

B. Expression of Na,K-Pump Isoforms

From the available information about the distribution and function of isoforms of α-subunit of Na,K-

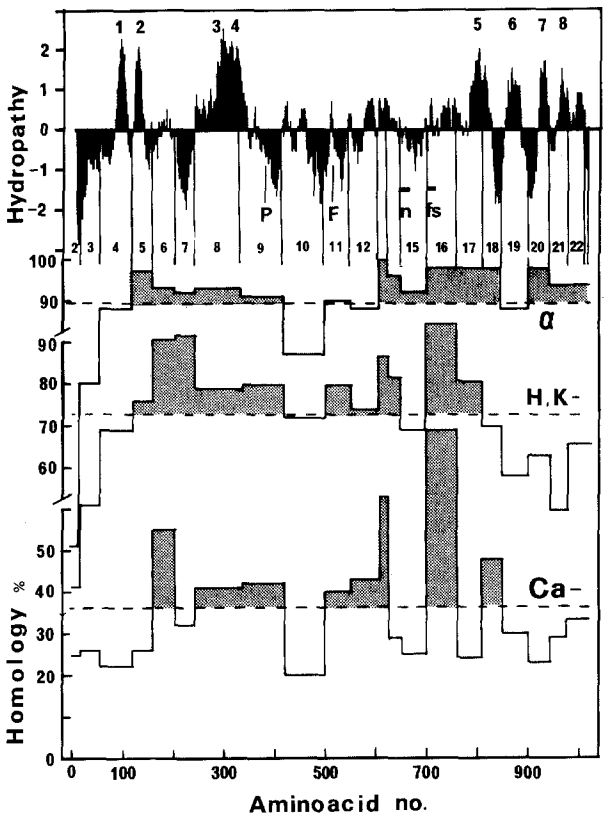

Fig. 3. Position of introns in the gene of α-III isoform [147] of Na,K-ATPase relative to a hydroplot of the amino acid sequence. Exons correspond to the numbers, and intron positions are marked with vertical lines. *M1–M8* refer to positions of transmembrane segments. Below the hydroplot the dotted lines show overall homologies and the columns show homologies of each exon in α-III isoform with α isoform [178], H,K-ATPase [180] and Ca-ATPase [19]. Since this figure is concerned with functional aspects, homologies include conservative substitutions (A–G, D–E, L–I, L–V, I–V, R–K, Q–N, S–T, Y–F)

ATPase it is already obvious that detailed analysis of the expression of isoforms using specific [^{32}P]-cDNA probes will reveal important new physiological and pathophysiological aspects of cation pump function in several tissues.

Three isoforms of Na,K-ATPase, α, α+, and α-III are identified from sequences of mRNA from rat brain [178]. Screening and sequencing of genes in human genomic libraries [147, 182] confirm that they are the products of separate genes. They do not have coding regions in common and restriction mapping of cDNA shows three distinct patterns in rat brain in contrast to predominance of the α isoform in rat kidney [210].

Overall homology is 97–98% between amino acid sequences of α isoforms of rat [178], sheep [179] or porcine [146] kidney, rat brain [178], and human HeLa cells [111], while it is 85–86% between α, α+ and α-III isoforms. The tertiary structural organization of the three isoforms is identical, but substantial differences amino acid sequence occur in the N-terminal region and in the region (exon 10 in Fig. 3) between the phosphorylation site (Asp-369) and Lys 501 that binds fluorescein-isothiocyanate (FITC). Close to 100% homology is found in ATP binding and phosphorylation segments and in the hydrophobic domains (M2, M5, and M7) (*cf.* Fig. 3 and Table 1). The N-terminal regions show considerable variation in number of charged residues and this may be important for catalytic differences between isoforms that can be related to different rates of E_1–E_2 transition [100].

The lower electrophoretic mobility of the α+ isoform under certain conditions [191] is not due to a higher molecular weight of α+ since it has fewer residues (1015) and lower M_r (111,736) than α (1018 res. and M_r 112,573) [178]. The catalytic properties of the α isoform are well known from studies on purified Na,K-ATPase from kidney [95], but the properties of α+ and α-III isoforms are uncertain since both forms are abundant in brain where the α+ isoform has been examined [170, 192]. It may therefore not be possible to distinguish their individual properties. In rats, the α+ isoform is more sensitive to digitalis than the α isoform and they differ in apparent affinity for Na^+ [120]. Their different properties [192] may be explained by different rates of E_1–E_2 transitions. Determination of the pattern of isoform distribution in a preparation may therefore be decisive for interpretation of results of kinetic experiments.

In whole kidney the ratio of α to α+ isoform is >280 : 1 [210] and only the α isoform seems to be present in thick ascending limb of Henle. It is likely that the small amounts of α+ mRNA in whole kidney is localized to cortical collecting ducts where Na,K-ATPase is more sensitive to digitalis than in other segments and subject to hormone regulation [44].

Hybridization of total RNA with cDNA probes, specific for each isoform, shows that the three known isoforms all are expressed in rat brain with α-III as the predominant isoform. The amount of α+ mRNA is high in skeletal muscle with a ratio of α+ to α mRNA of 30 : 1. The α+ isoform is also found in heart muscle, adipose tissue, stomach and lung, whereas α-III is detected in brain, stomach, and lung [210]. It is interesting to note the distribution of isoforms in heart muscle, where the level of α+ isoform is greater than α isoform in ventricles, while the converse is true for atria where the α isoform predominates [210]. This may form the basis for the pronounced sensitivity to digitalis of the hypertrophied heart since there are increased amounts of α+ isoform in the ventricles [124].

In brain the α and $\alpha+$ isoforms have a characteristic cellular distribution that may be of importance for function. The α isoform occurs in astrocytes and unmyelinated sympathetic neurons while $\alpha+$ predominates in myelinated neurons [171, 186]. Quantitation with antibodies and labeling with FITC show that the $\alpha+$ isoform increases more rapidly than the α isoform during brain development, but development of both forms depends on regulation by thyroid hormone [169]. In the salt gland of the Brine shrimp two isoforms were identified as translation products of two mRNA's, but the structural relationship of these isoforms to those in brain is not known [59]. Two noninteracting pools of isozymes with high and low affinity for ouabain and different sensitivity to alkylation of sulfhydryl groups are found in the salt gland of *Squalus acanthias* [128]. The functional significance of this appearance of $\alpha+$ isoforms in epithelial cells is unknown.

C. Gene Expression of β-Subunit

Isoforms of β-subunit are not identified as yet, but hybridization analysis with [^{32}P]-cDNA identified multiple β-subunit cDNA forms, that all appear to code for a single β-subunit protein [211]. The β-subunit mRNA is identified in all tissues where α-subunit mRNA is found, but their relative levels vary considerably [87]. In kidney and brain, the levels of α and β mRNA are similar, while α mRNA levels are sixfold greater than β mRNA in muscle and lung; in stomach the reverse is true [210].

Studies on neuronal cells show that synthesis of α-subunit and β-subunit are concurrent and that assembly of the $\alpha\beta$-unit of Na,K-ATPase occur during or immediately after polypeptide synthesis [195]. Coordinate synthesis is also observed in myogenic cells [207] and epithelial cells of toad bladder [66].

Transfection of β-subunit from avian cells with high ouabain affinity and expression in the cell surface of mouse cells with relatively low affinity receptors for ouabain shows that ouabain sensitivity does not follow the β-subunit. The transfected mouse cell line expresses the avian β-subunit of Na,K-ATPase from an uncontrolled promotor. This cell line will therefore provide an interesting tool for examining control of gene expression in situations where the cells regulate their content of Na,K-ATPase up or down in response to altered concentrations of Na in the cell cytoplasm [56].

D. Structure and Expression of Ca-ATPase Genes

In rabbit genomic DNA there are two genes corresponding to the slow and fast forms of sarcoplasmic reticulum Ca-ATPase that have been characterized in biochemical experiments. This agrees with the observation that the basis for Brody's disease is a diminished capacity for relaxation of skeletal muscle in fast but not in slow twitch skeletal muscle [19].

The messenger transcripts of the two genes are different, the fast twitch mRNA being smaller than that of the slow twitch. Both 5′ and 3′ nontranslated regions are widely divergent in sequence and thus useful probes for differentiating mRNA and cDNA coding for the two forms of Ca-ATPase.

The neonatal and adult isoforms of fast Ca-ATPase are expressed by alternative splicing of an exon. A 42-bp exon is retained in adult and excised in neonatal transcripts causing expression of fast Ca-ATPase with different carboxyl termini [20]. Slow Ca-ATPase is expressed in adult slow twitch muscle and in cardiac muscle. The slow form has lower ATPase activity than the fast form. The presence of the regulatory molecule phospholamban and effects of calmodulin in cardiac and slow twitch fibers suggests that slow Ca-ATPase is subject to regulation [91, 193]. It is interesting that the fast isoform of Ca-ATPase shows more sequence homology with the α isoform of Na,K-ATPase than does the slow isoform. Conversely, the slow isoform of Ca-ATPase shows higher homology with the $\alpha+$ isoform of Na,K-ATPase that is often found in cells where the pump seems to be under regulation of hormones or secondary messengers [120].

E. Order of Gene Expression of Cation and Phosphorylation Sites in KdpABC

Studies of mutations of the Kdp operon in *Escherichia coli* may be relevant for understanding expression and structure of other cation pumps. Three proteins are coded by the genes of the Kdp operon, KdpA (M_r 59,189), KdpB (M_r 72,112) and KdpC (M_r 42,510) [52, 82]. They are expressed in *E. coli* only when [K^+] falls below 15 mM. Pumps with reduced affinities for K^+ but unaffected maximum rates of active K^+ transport have mutations only in Kdp A [43]. This hydrophobic protein may form sites for K^+ binding that are separate from domains in KdpB for binding of ATP and phosphorylation. The Kdp operon is transcribed in the order A before B and C [52]. If this order is conserved in evolution one can draw the interesting conjecture that the cation binding domain will be N-terminal to the phosphorylated domain in a cation pump consisting of a single subunit.

These mutations may also provide information about the stoichiometry of the Kdp K-transport complex [52]. Two missence mutations of KdpA

near the N- and C-terminus, respectively, are complementary. The molar ratio of the subunits is close to one and the intracistronic complementation may therefore provide evidence that the gene product of Kdp A, B, and C is present as a dimer.

F. Gene Regulation and Biosynthesis

The amount of Na,K-ATPase in cell membranes is modulated according to the demand for transport capacity through effects of Na^+ concentrations in cytoplasm on transcription or biosynthesis rates. This feedback regulation of the amount of Na,K-ATPase protein in the cells was proposed as a hypothesis for explaining adaptive changes in amount of Na,K-ATPase following changes in supply of Na to adrenalectomized rats [92]. In this model a sustained change in Na/K ratio in cytoplasm following an increased influx of Na^+ results in adaptive increases in amount of Na,K-ATPase that appear slowly after 16–24 hr in vivo. The increased transport capacity in the cell subsequently restores cytoplasmic Na/K activities to original levels, thus completing the feedback cycle. The mechanism for the effect of Na/K ratio on synthesis of $\alpha\beta$-unit of Na,K-ATPase is not clarified, but recent quantification of mRNA by hybridization with [^{32}P]-cDNA shows an early rise in amount of specific mRNA followed by a late increase in rate of synthesis of the α-subunit and β-subunit and in abundance of $\alpha\beta$-unit in the cells [17, 158]. Also in muscle [207] and in suspensions of kidney tubule cells [160] it can be demonstrated that an increase in Na/K ratio after 2–4 hr triggers a marked increase in rate of synthesis of Na,K-ATPase protein. The time required for affecting a change in amount of Na,K-ATPase (16–24 hr) agrees with the rate of change in response to in vivo changes in Na^+ load. Rates of degradation of $\alpha\beta$-unit are slow with $T_{1/2}$ = 20–40 hr.

It has been proposed that an elevated cytoplasmic Ca^{2+} concentration leads to increased synthesis of Ca-ATPase and other muscle proteins by an effect at the transcriptional level, mediated by nuclear Ca^{2+} binding proteins [127], but direct experimental evidence has not appeared.

Mechanisms for direct hormone effects on biosynthesis rates have not been resolved. In principle, hormones may act on transcription or translation of mRNA, on recruitment of an intracellular pool or via changes in cytoplasmic cation concentrations. Aldosterone effects on the rate of mRNA synthesis have been analyzed in relation to stimulation of Na,K-ATPase synthesis [201]. In cortical collecting ducts, aldosterone increases the amount of Na,K-ATPase by *de novo* synthesis of pump units independent of changes in cytoplasmic Na^+, while changes in Na^+ concentration may stimulate recruitment of a latent pool of Na,K-ATPase independent of protein synthesis [44]. An intracellular pool amounting to 30–70% of total Na,K-ATPase has been demonstrated in muscle cells [207] and cultures [17, 195].

IV. Organization of the Cation Pump Proteins in the Membrane

Presumptive membrane-spanning segments can be identified in the amino acid sequences, but the availability of the amino acid sequences of the cation pumps has not led to solution of the overall topology of the lipid-associated domains. Biochemical studies, such as selective proteolytic or chemical cleavage in combination with specific chemical labeling from the membrane surfaces or the hydrophobic interior, are required to determine the orientation of intramembrane segments and the sidedness of N- and C-terminal segments. It is important to evaluate whether the topology of the membrane protein as determined from these data correlates with the distribution of mass between extra- and intramembranous domains as estimated in models derived from physical studies of membrane crystals.

A. Insertion in Endoplasmic Reticulum Membrane

Information about the mechanism of biosynthesis may help to establish the orientation of N- and C-termini of the pump proteins. Orientation of the membrane protein in endoplasmic reticulum is conserved during transport to the surface cell membrane and in maturation of sarcoplasmic reticulum so that domains exposed on the luminal side in ER are eventually exposed on the noncytoplasmic side. The subunits of Na,K-ATPase [195] and Ca-ATPase [122, 132] are synthesized without a cleavable hydrophobic N-terminal signal sequence, yet they are cotranslationally inserted into the endoplasmic reticulum membrane due to the presence of insertion signals further down the sequence. In vitro expression of deletion mutants of cDNA of human α-subunit and β-subunit shows that membrane insertion signals are contained in M1–M4 in α-subunit [86] (*cf.* Figs. 1 and 3). The presence of one of these segments is required for insertion of α-subunit in the membranes of an in vitro biosynthesis system. Insertion of β-subunit is possible as long as at least 16 residues in the transmembrane segment (Res. 34–53).

The cation pump proteins belong to a group of transmembrane proteins with the N-terminus exposed on the cytoplasmic surface [85]. Multiple

crossings can be generated by a sequence of alternating cotranslational insertion and halt transfer signals [166]. Cotranslational insertion signals span the membrane from cytoplasm to noncytoplasmic surface in the N-C direction. The hydrophobic part of a halt transfer signal would span the membrane with opposite direction. The location of the C-terminus during insertion of the membrane protein in the ER membrane will thus depend on whether the last transmembrane segment serves as part of an insertion or halt transfer signal. In agreement with this scheme studies of the structure of Na,K-ATPase [95] and sulfhydryl modification of Ca-ATPase [161] shows that their N-termini are cytoplasmic, while localization of their C-termini is uncertain (*cf.* pp. 106 and 107).

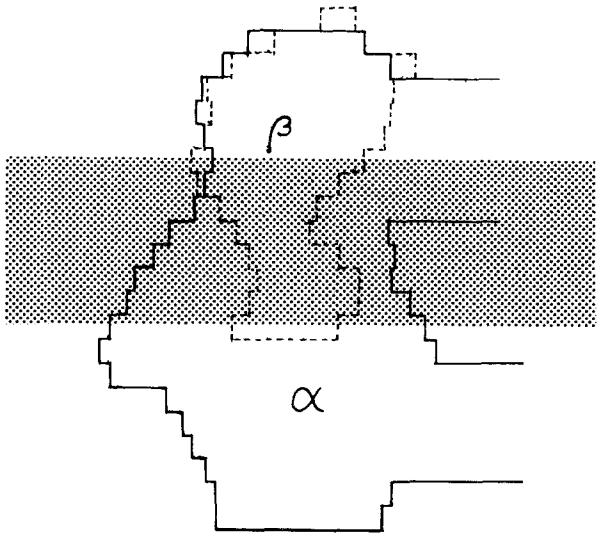

Fig. 4. Model of distribution of protein mass of $\alpha\beta$-unit between extra- and intramembranous domains. The position of the bilayer corresponds to the shaded area. Redrawn from models of $\alpha\beta$-unit by Hebert et al. [80] and model of a crystal of the β-subunit [148]

B. Crystallization in the Membrane

The very dense packing of asymmetrically oriented protein in purified membrane-bound Na,K-ATPase from kidney allowed crystallization of the pump protein in the membrane by incubation in vanadate medium [79, 95, 102, 183, 212]. This procedure also induces formation of crystalline arrays of Ca-ATPase in sarcoplasmic reticulum [50, 197] and in preparations of H,K-ATPase from stomach mucosa [159]. Initially type p1 crystalline arrays with unit cells consisting of monomeric $\alpha\beta$-units were observed in Na,K-ATPase, but later more scarce and infrequent p21 crystal forms consisting of dimeric $(\alpha\beta)_2$-unit cells were identified [79, 102, 144, 212]. The high rate of crystal formation of protein in the E_2-form in vanadate solution [102, 183] shows that the E_1–E_2 transition in the pump protein alters conditions for interaction between subunits in the membrane. In Ca-ATPase the vanadate-induced crystals represent E_2 forms while crystals induced by Ca^{2+} or lanthanide represent the E_1 form of the enzyme [50]. This simple relationship between conformational state and crystal form is not seen in preparations of Na,K-ATPase, where both p1 and p21 crystal forms develop in vanadate medium.

It is noteworthy, that the minimum asymmetric unit cell in the crystals of the Na,K-pump and the Ca-pump contains the same protein unit as the minimum functional unit of soluble Na,K-ATPase ($\alpha\beta$-unit) and Ca-ATPase (*cf.* Section VI).

C. Three-Dimensional Models

Low resolution models (20–30 Å) made after diffraction analysis of membrane crystals of Na,K-ATPase [80, 131, 144] and Ca-ATPase [24, 197] show that cytoplasmic protrusions of the proteins are remarkably similar. A notable difference is a 10–20 Å protrusion on the extracellular surface of the model for Na,K-ATPase while the Ca-ATPase model has a smooth extracytoplasmic surface. Superposition of a model of β-subunit crystals formed in Mg solution shows that the β-subunit forms the extracellular protrusion [148], as shown in Fig. 4. This agrees with estimates of distances in fluorescence studies [118]. The mass of the intramembranous portion [80] estimated from this $\alpha\beta$-unit model is 30 to 40% of the total mass of the three-dimensional model of the $\alpha\beta$-unit. Similarly, estimates of intramembranous portion of Ca-ATPase are in the range of 30–50% [197].

The relatively low resolution (25 Å) of these models does not allow further assignment of structural detail. This requires preparation of crystals suitable for X-ray crystallography. Methods developed for photosynthetic reaction center [38] have not been directly applicable to other membrane proteins. Recently, small three-dimensional crystals consisting of sheets of protein arrays separated by lipid layers, were prepared from soluble Ca-ATPase in nonionic detergent [49], but the crystals are fragile and not yet suitable for X-ray analysis. A critical factor for formation of these crystals is stabilization of the soluble protein in an enzymatically active form for several months.

D. Mass of Intramembrane Protein

In agreement with the estimate from crystal models, diffraction studies on oriented multilayers of sarco-

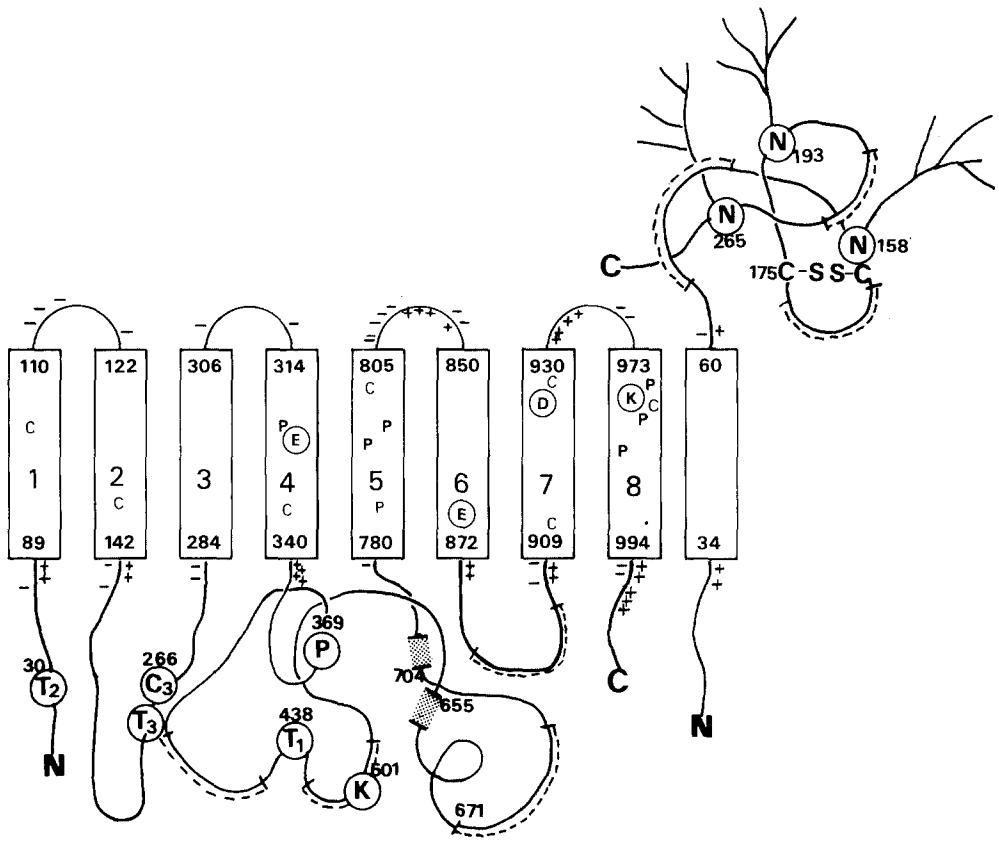

Fig. 5. Disposition of $\alpha\beta$-unit in the membrane, based on sequence information [111, 112], labeling with FSBA [33, 141], and selective proteolytic digestion of α-subunit [100]. Model for β-subunit is based on sequencing of surface peptides [130, 141] and identification of S-S bridge [142]. T_1, T_2, T_3, and C_3 show location of proteolytic splits. *N* are glycosylated asparagines in the β-subunit. (+) and (−) indicate all extracellular charged residues and charges within the first 10 residues from the transmembrane segments at the cytoplasmic face. (⊣▒▒⊢) shows FSBA labeling and (═══) segments located at the protein surface [141]

plasmic reticulum show that about 40% of the Ca-ATPase peptide mass is distributed within the hydrophobic core of the membrane [16]. An alternative estimate of mass distribution is obtained by proteolysis. Extensive digestion with excess trypsin or unspecific proteases shows that 40–50% of the protein of Na,K-ATPase [105] or Ca-ATPase [208] is protected by lipid or secondary structures that are resistant to proteolysis.

Calculation of mass distribution of the model in Fig. 5 with eight transmembrane segments in α-subunit and one in β-subunit shows that 27% of $\alpha\beta$-unit mass is extracellular, 58% is exposed on the cytoplasmic surface and only 15% of $\alpha\beta$-unit mass is inside the membrane. The 10 hydrophobic segments proposed to traverse the membrane in the model of Ca-ATPase [19] constitutes about 20% of the protein mass.

These data show that the mass of 8 + 1 or 8 − 10 transmembrane segments in Na,K-ATPase or Ca-ATPase, may be less than the mass of intramembrane protein determined by other methods. With this in mind it is appropriate to consider the possibility that the cation pumps possess intramembrane protein structures in addition to those of predicted transmembrane helices.

E. Paradigms for Secondary Structure of Intramembrane Protein

Combined knowledge of sequence and structure at high resolution is available only for the photosynthetic reaction center of bacteria [38, 129]. The amino acid sequences of three subunits fit well into the electron density map based on X-ray crystallography with identification of individual residues. A total of 11 transmembrane structures is found typically consisting of α-helices of 19–23 amino acid residues without basic or acidic side chains. Using a window of 19, the hydroplot analysis [117] shows that four of the helices have a hydrophatic index peak above 2.0 and another four have a peak above 1.5, while three have index peaks between 1 and 1.5.

Formation of β-sheet in integral membrane proteins has been predicted in porin and gap junction protein [151, 152] and X-ray diffraction measurements reveal a transmembrane domain with a high proportion of β-sheet running parallel to the membrane surfaces in gap junction [125]. In a β-sheet structure an extensive network of hydrogen bonds may allow polar residues to exist in environments of low dielectric constants [12]. Only 10 residues may be required to traverse the hydrophobic membrane core in an extended β-configuration of a polypeptide. Porin spans the outer membrane lipid bilayer of *E. Coli* to form voltage-dependent channels in a compact structure with little material protruding into the aqueous phase [151], but hydroplots of its protein shows at most one sizeable hydrophobic domain with a hydrophatic index above 1.5.

Another possibility for explaining the presence of both hydrophobic and polar or ionizable residues within the membrane is the packing in amphipathic helices possessing hydrophobic nonpolar faces and relatively narrow charged polar faces in helical wheel plots [*cf.* 19]. Critical evaluation of algorithms for predicting secondary structure shows that they are inadequate for membrane proteins, particularly when used on hydrophobic segments [206]. As an example, secondary structure prediction according to Chou and Fassmann [30] of the photosynthetic reaction center [38] shows higher propensity for β-sheet than for α-helix for hydrophobic segments that are indeed organized in α-helical structures in the high resolution model from X-ray crystallography.

F. Intramembrane Structure of Na,K-ATPase

In the model of the α subunit of Na,K-ATPase in Fig. 5, the transmembrane segments M1, M2, M3, M4, and M5 are predicted by a hydrophatic index of >2.0 and three segments M6, M7, and M8 have a peak index of >1.5 using a window of 19 residues for the hydroplot [116]. These segments consist of 21–25 amino acid residues with over-representation of the hydrophobic residues Phe, Ile, Leu, Val, Trp, Tyr, but also of Pro and Cys. This may suggest that S-S bridge formation is part of stabilizing intramembrane structures. Prolines break the continuity of membrane helices and the excess of proline is interesting in view of a recent survey demonstrating membrane-buried proline residues in transport proteins, while they are excluded from the membranous domains in nontransport proteins [18]. *Cis-trans* isomerizations of peptide bonds involving proline may thus be part of the conformational transitions associated with the transport process. Few basic or acidic side chains are found in the transmembrane segments in Fig. 5, but the segments carry charged residues close to their cytoplasmic ends. These charges may react with headgroups of lipids to stabilize the structure in the membrane [21, 54]. During biosynthesis the charged residues may have served as stop signals [166], preventing transfer across the membrane.

The presence of four transmembrane segments in the N-terminal half of the α-subunit of Na,K-ATPase was predicted from the results of controlled tryptic cleavage combined with selective chemical labeling with photosensitive ouabain, phosphorylation [95, 102] and insertion of small hydrophobic probes, [^{125}I]-iodonaphtylazide (INA) [15], [^{125}I]-trifluoromethyl-iodo-phenyldiazirine (TID) [23, 99], or [^{3}H]-adamantane diazirine [139]. In contrast, neither chemical labeling experiments nor hydroplot analysis lead to a decision as to whether 2, 4, or 6 transmembrane segments are formed by the C-terminal part of the α-subunit (Res. 779-1016) and orientation of the C-terminus remains uncertain. Recent immunological studies suggest the presence of an extracellular epitope near the C-terminus of α-subunit [130]. This leads to a model with only seven transmembrane segments in the α-subunit.

Possible candidates for additional intramembrane structures in the α-subunit are relatively hydrophobic segments with high β-sheet propensity in the cytoplasmic domains, e.g. segments 175–202, 242–260, 410–430, and 560–590 in α-subunit (Fig. 5, [181]). These segments alternate with α-helices and may form flexible structures that contribute to cation binding and E_1–E_2 transition.

G. Intramembrane Structure of Ca-ATPase

A similar ambiguity exists regarding the disposition of transmembrane segments of the Ca-ATPase peptide chain including sideness of the C-terminus. A model of Ca-ATPase with 10 transmembrane segments [19, 121] is based on plots of polarity index. Hydroplots with a window of 19 as described above reveals four to five rather than six transmembrane segments in the C-terminal portion (*cf.* Fig. 1). The proposed α-helical structure of the transmembrane segments is consistent with circular dichroism measurements on the part of the protein left attached to the membrane after extensive tryptic digestion [73]. In addition to these transmembrane segments, the Ca-ATPase sequence contains more hydrophobic stretches, e.g. res. 210–230 and part of the surface of presumptive amphipathic helices [19]. The amphipatic helices connect the transmembrane segments M1–M5 with the cytoplasmic domains. They have been implicated in formation of a "stalk" seen

by negative staining, but "lollipop" structures are absent in vanadate-treated enzyme [31]. This could mean that the amphipatic helices are membrane embedded, at least in the E_2 form, adding about 10% to the intramembranal mass.

V. Structure of β-Subunit of Na,K-ATPase

With the possible exception of the KdpC protein of K-pump [82] and a glycoprotein in the sarcoplasmic reticulum [119], the presence of a glycoprotein like the β-subunit is unique for Na,K-ATPase in the family of cation pumps. Sequences of β-subunit (302 residues, M_r 34.528) are now available from human HeLa cells [112], sheep [179], pig [146] and dog [22] kidney and *Torpedo electroplax* [140]. The initiating methionine is removed in posttranslational processing, but otherwise the NH_2-terminal sequence from cDNA is identical to that determined by gas phase sequencing [22, 100].

The bulk of hydrophilic residues of β-subunit are exposed on the extracellular surface [51]. The β-subunit sequence has one hydrophobic segment (res. 34–53) with hydropathic index above 2.0 that may form a transmembrane helix. This is basis for the model in Fig. 5. The β-subunit is labeled from the bilayer by [^{125}I]-iodonaphtylazide [105] and [^{125}I]-trifluoromethyl-iodo-phenyldiazirine [101]. As alternative to this model three transmembrane segments are proposed on basis of papain digestion [29] and immunological studies [213], but there is no evidence for this in hydroplots of the sequence.

The β-subunit is not as well conserved as the α-subunit, with 91% overall homology between β-subunit of sheep, pig, and human and 61% between β-subunit of human and *Torpedo*. This might suggest a dissociation in development between α-subunit and β-subunit, but closer inspection reveals a wide variation in conservation. Some segments are invariant among mammalian, avian and piscine β-subunits like the best conserved segments of α-subunit. This applies to the N-terminus (res. 1–94) and C-terminus (res. 235–302) and the location in the sequence of three glycosylation sites, seven cysteins and four tryptophans. In other domains, sequence homology is low, e.g. the sequences around the 1st (N-157) and 2nd (N-192) glycosylation sites show less than 50% homology in alignment among the mammalian species. An S-S bridge is detected between Cys 158 and Cys 175 [142] that may be essential for Na,K-ATPase activity [53, 113]. These observations suggest that certain segments of β-subunit may be important for Na,K-ATPase function, e.g. for proper insertion of the α-subunit in the membrane during biosynthesis, while the less conserved parts are of purely structural importance. Otherwise the appearance of the amino acid sequence data have not relieved our lack of understanding function of the β-subunit.

VI. Soluble Protomeric Na,K-ATPase and Ca-ATPase

After gradual refinement of techniques for solubilization and chromatography, reliable data defining the mass and subunit structure of cation pump proteins have become available [13, 95, 126, 132]. Molecular weights of the soluble enzymes as determined by sedimentation equilibrium and sedimentation velocity studies [8, 98] agree with those calculated from amino acid composition with ±10% (110,458 for Ca-ATPase and 147,000 for αβ-unit of Na,K-ATPase). Sedimentation coefficients are 5 S for monomeric Ca-ATPase and 6–7 S for the protomeric αβ-unit of Na,K-ATPase. Fluorescence energy transfer depolarization [84] also indicate a monomeric state of soluble Ca-ATPase. High resolution gel chromatography combined with low angles laser light scattering gives molecular weights for soluble Na,K-ATPase [77] that are in agreement with those from sedimentation equilibrium analysis. Monomer Ca-ATPase elutes with full activity from the columns [6, 8] and the soluble monomer while passing down the column carries Ca^{2+} in the occluded state [8, 202].

Soluble Na,K-ATPase undergoes time-dependent denaturation and aggregation as a function of temperature and cation composition of the medium [98]. High resolution chromatography rapidly inactivates soluble Na,K-ATPase, but the addition of phosphatidylserine [78] allows assay of Na,K-ATPase activity during passage over the TSK column. This experiment confirms that protomeric αβ-units have Na,K-ATPase activity.

The monomeric Ca-ATPase and the protomeric αβ-unit of Na,K-ATPase constitute the minimum functional units required for all aspects of the reaction cycle including E_1–E_2 and E_1P–E_2P transitions [3, 5, 98] and occlusion of Ca^{2+}, Na^+, and Rb^+/K^+ [202, 203]. For monomeric Ca-ATPase, the stoichiometry for phosphate or vanadate binding and Ca^{2+} occlusion is the same as for the membranous enzyme [4–6, 8, 202]. Soluble protomeric Na,K-ATPase binds one molecule of ATP [90] or ouabain [143] and the αβ-unit is capable of occluding Rb^+ (K^+) or Na^+ with the same stoichiometry relative to maximum phosphorylation as the membrane-bound enzyme [203]. From a structural point of view it is

particularly important that a cavity for occlusion of the cation is formed within protomers both in membranous and soluble state. The properties of the occluded complexes discussed below show that a cavity for occlusion is a part of the cation transport pathway across the membrane. Formation of an occlusion cavity within the protomer therefore suggests that this is the minimum protein unit required for active Ca or Na,K transport. Direct evidence for a protomer cation pump has been obtained for H-ATPase [71].

VII. Cytoplasmic Domains and Ligand Binding Areas

A characteristic structural feature of the cation pump proteins is a cytoplasmic protrusion with approximate dimensions 45 × 65 Å in the plane of the membrane and a length of 50–60 Å in the plane perpendicular to the membrane. As illustrated in Fig. 5, the transmembrane segments separate the protrusion into subdomains. Selective cleavage and chemical labeling established structure-function correlates for some of these domains. The bulk of the protrusion is formed by the large central domain (res. 340–780 in α-subunit and 309–758 in Ca-ATPase) that forms sites for ATP binding and phosphorylation. The second cytoplasmic domain (142–284 in α-subunit and 108–256 in Ca-ATPase) between M-2 and M-3 contains peptide bonds susceptible to proteolytic cleavage in E_1 forms. The N-terminus is attached to M-1 and is important for control of E_1–E_2 transition in Na,K-ATPase and of the rate of Na,K-pumping, but the N-terminus may not have such a role in Ca-ATPase.

A. Sites for Nucleotide Binding and Phosphorylation in Na,K-ATPase

The segments contributing to nucleotide binding and phosphorylation domains undergo structural changes accompanying E_1–E_2 transition as the ATP binding region adapts for tight binding in the E_1 form with K_d 0.1 μM [90], while binding to the E_2 form is weak requiring millimolar concentrations of ATP for saturation. In addition, structural [102] evidence suggest that motion of the phorphorylated residue may be part of the transition from E_1 to E_2. Studies of other ATP binding proteins show that functional residues are contributed by regions of different protein sequences and secondary structure. An indication of the functional groups required to form a nucleotide site may be obtained from examining sites in dehydrogenases [165], phosphofructokinase [114] and, in particular, adenylate kinase [64].

An important feature is a hydrophobic pocket for accommodation of the adenine and ribose moieties which is formed by Ile, Val, His and Leu residues. The triphosphate moiety is flanked by a hydrophobic strand of parallel β-pleated sheet terminated by Asp [64]. As seen from Table 1*c*, such a segment in adenylate kinase and β-subunit of F1-ATPase shows some homology with respect to charges and hydrophobic residues to segments in α-subunit of Na,K-ATPase (543–561) and Ca-ATPase (612–628). The N-terminal part of this segment is rich in glycines and may form a flexible loop that undergoes conformational transitions related to altered affinity of the site or to reallocation of catalytic groups [*cf.* 64]. In adenylate kinase, other segments contribute an α-helix with hydrophobic residues separating two lysines that may interact with phosphate moieties.

In addition to the segment around Asp 369 (Table 1*a*), labeling with ATP analogues provides evidence for contribution from three additional segments in α-subunit of Na,K-ATPase. The first indication came from ATP-sensitive covalent insertion of FITC into Lys-501 in α-subunit [104]. FITC also inserts covalently in Ca-ATPase of SR [155], in Ca-ATPase of erthrocyte membranes [58] and in H,K-ATPase [180], (Table 1). The strong fluorescence signal provides a convenient probe for monitoring conformational transitions in the proteins. Fluorescein is a relatively large molecule and the specific insertion at Lys-501 does not necessarily indicate that this residue also forms part of the nucleotide binding area.

The C-terminal part of the central domain contributes two peptide segments (655–664 and 704–722) that are labeled by FSBA [141] 5-(*p*-fluorosulfonyl)-benzoyl-adenosine, an ATP analogue that labels the Na,K-ATPase with concomitant inhibition of ATP hydrolysis, while K-phosphatase and ouabain binding remain intact [33]. The peptides are located at residues 655–664 and 704–722 of the α-subunit. Another ATP analogue, γ-[4-(N-2-chlorethyl - N - methylamino)]benzoylamid - ATP (CIR-ATP) inserts covalently in Asp-710 in the 704-722 segment [149]. Labeling by these ATP analogues may relate to charged residues coordinating phosphate moieties in ATP.

Peptides released from the surface of the central domain of the α-subunit by tryptic cleavage have also been sequenced [141] and a provisional arrangement of the ATP binding domain in the cyto-

Table 1. Sequence homologies of nucleotide binding and phosphorylation domains[a]

Res. no.		
a) Phosphorylation domain		
367	T S T I C S D K T G T L T Q N R M	Na,K,α
379	T S V I C S D K T G T L T Q N R M	H,K-
345	T S V I C S D K T G T L T T N Q M	Ca-
372	V E I L C S D K T G T L T K N K L	H-, yeast
301	V D V L L L D K T G T I T L G N R	KdpB
273	L D V I M L D K T G T L T Q G K F	K-, *S.f.*
280	Q E R I T S T K T G S I T S V Q A	F1-, β, *coli*
293	Q E R I T T T K K G S I T S V Q A	F1-, β, bov.
b) FITC reactive region		
496	P Q H L L V M K G A P E R I L D R C S S	Na,K,α
510	P R H L L V M K G A P E R V L E R C S S	H,K-
508	V G N K M F V K G A P E G V I D R C N Y	Ca-
	M Y S K G A S E I I L R	Ca-p.m.
467	G E R I V C V K G A P L S A L K T V E E	H-, yeast
467	G E R I T C V K G A P L F V L K T V E E	H-, *Neurosp.*
388	I D N R M I R K G S V D A I R R H V E A	KdpB
c) Nucleotide-binding region		
543	L G E R V — L G F C H L F L P D E Q F P	Na,K-,α
613	L K C R T — A G I R V I M V T G D H P I	H,K-
611	Q L C R D — A G I R V I M I T G D N K G	Ca-
544	C E A K T — L G L S I K M L T G D A V G	H-, *Neurosp.*
545	S E A R H — L G L R V K M L T G D A V G	H-, yeast
243	E Y F R D Q E G Q D V L L F I D N I F R	F1-, β, bov.
267	E Y F R D — R G E D A L I I Y D D L S K	F1, α, *coli*
277	V L — R G N G G A F V L V L Y D E I K K	ATP-ADP exch.
104	E F E R K — I G Q P T L L L Y V D A G P	Aden. kin.
87	E Q L K K — H G I Q G L V V I G G D G S	Phosphofr.
d) Segment binding FSBA and Cl-ATP in Na,K-ATPase		
703	Q G A I V A V T G D G V N D S P A L K K	Na,K-,α
717	L G A I V A V T G D G V N D S P A L K K	H,K-
694	Y D E I T A M T G D G V N D A P A L K K	Ca-
625	R G Y L V A M T G D G V N D A P S L K K	H-, *Neurosp.*
625	R G Y L V A M T G D G V N D A P S L K K	H-, yeast
509	E G R L V A M T G D G T N D A P A L A Q	KdpB
467	Q G K K V I M V G D G I N D A P S L A R	K-*S.f.*

[a] References to sequences: Na,K-ATPase, α subunit [111], H,K-ATPase [180], Ca-ATPase [19], Ca-ATPase pl. m. [58], H-ATPase, yeast [177], H-ATPase, *Neurospora* [1], KdpB [82], K-ATPase, *S. faecalis* [185], F1-ATPase, β, *E. coli* and bovine [205], ADP-ATP exchange [10], adenylate kinase [64], phosphofructokinase [114]. Labeling with FSBA [141] and Cl-ATP [149].

plasmic protrusion has been drawn as in Fig. 5 without attempts to illustrate molecular detail of the binding site.

B. Nucleotide Site of Ca-ATPase

In addition to the segments identified in Table 1, nucleotide-specific reactions show that other residues are involved in ATP binding. Trp-552 is the only tryptophan residue in the central domain and efficient energy transfer to bound nucleotides suggests that it may be located close to the nucleotide binding area [27, 135]. Cys-674 can be modified with fluorescent and spin-label derivatives of iodoacetamide showing nucleotide-induced spectral changes [11, 32, 187, 209]. N-iodoacetyl-N'-(5-sulfo-1-naphtyl) ethylenediamine (IAEDANS) bound at Cys 674 has been localized as much as 50–60 Å from the FITC site and only 16–18 Å from Ca sites. It is suggested that Ca sites are N-terminal to the site for insertion of FITC and that the two subdomains are folded onto each other, each forming the wall of a cleft containing the bound ATP [187] with FITC and IAEDANS sites being located at the ends. The rapid primary tryptic cleavage at T_1 (Arg

505) is independent of conformation, but ATP binding stabilizes interaction between the tryptic fragments after cleavage at Arg 505 and also prevents cross-linking of the fragments with glutaraldehyde [48, 164]. The data agree with the notion that T_1 divides the central cytoplasmic segment into two subdomains (res. 309–505 and 506–758).

C. Cation Sites

The problem of assigning Na^+, K^+ or Ca^{2+} binding sites to residues in the amino acid sequences has not been solved. It will also be important to learn if cation sites are located in the cytoplasmic protrusion or if they are part of the intramembrane portion of the pump protein. Studies of cation binding at equilibrium (for ref. *see* 95) and competition between Na^+ and K^+ for binding and occlusion (62, 102] are in agreement with the notion that the Na,K-pump possesses a single set of sites for binding of either Na^+ or K^+.

Stabilization of occluded E_1 or E_2 forms of the protein allows detailed examination of loading and unloading of cation sites under the influence of specific ligands, but cation sites have not been identified in α-subunit or β-subunit sequences. N,N′-dicyclohexylcarbodiimide (DCCD) inhibits Na,K-ATPase in a Na^+- or K^+-dependent manner suggesting that it binds to carbonyls that are essential for activity, but inactivation may be due to crosslinking by formation of intrapeptide bonds rather than modification of specific carboxyls that are part of cation sites [72, 153].

The peptide chain of Ca-ATPase in the E_1 state forms two cytoplasmic high affinity sites for Ca^{2+} ($K_{0.5}$ 0.1–1 μM). Binding isotherms show evidence of positive cooperativity and the dissociation of the two Ca^{2+} ions occurs in an ordered way as measured in isotope exchange experiments [46, 137]. This indicates that the two sites are nonequivalent because one Ca^{2+} ion sterically hinders access of the other to solvent.

Examination of known site structures of various Ca^{2+}-binding proteins indicates that high affinity requires 6–7 coordinating protein oxygen atoms per Ca^{2+} ion, including several carboxyl groups [204]. NMR and luminescence studies with lanthanide ions indicate that the first coordination sphere of bound ion contains as little as 1–3 water molecules [172, 189]. Transformation of E_1Ca_2 to the occluded $E_1P[Ca_2]$ form and thereafter to the low affinity E_2PCa_2 form probably involves changes of the number of coordinating groups and of the state of hydration of Ca^{2+} [189, 196]. Redistribution of coordinating groups as part of E_1–E_2 transition is suggested from the observation of a larger number of low affinity Ca^{2+} sites on the extracytoplasmic surface in E_2 forms relative to E_1 forms [75].

Although the sequence data do not indicate the existence of a classical EF-hand Ca^{2+} site, studies with monoclonal antibodies show that there may be a site on Ca-ATPase with a similar tertiary structure as the EF-hand sites [214]. Carboxyl groups are present at a high density in the N-terminal quarter of the Ca-ATPase peptide and some of those located on A2 (res. 1–198) can be protected from carbodiimide labeling by Ca^{2+} [26, 156]. The putative Ca^{2+} sites identified by carbodiimide labeling are located close to or within the lipid bilayer and at a long distance (40–50 Å) from the FITC binding site as measured in fluorescence energy transfer studies [173, 174]. The distance between the two Ca^{2+} sites is only about 10 Å [173]. The suggested amphipatic helices connecting transmembrane segments in the N-terminal region with cytoplasmic segments have been implicated in formation of Ca^{2+} sites [19]. It has been proposed that ion movement and affinity changes in relation to the E_1–E_2 transition should be understood in terms of twisting and realignment of these helices [19].

VIII. Structural E_1–E_2 Transitions Detected by Proteolytic Cleavage

Exposure and protection of bonds on the surface of the cytoplasmic protrusion provides unequivocal evidence for structural changes in α-subunit accompanying E_1–E_2 transition in Na,K-ATPase [93, 95]. This provided a short cut to identification of residues involved in E_1–E_2 transition [100] and to detection of structure function relationships [102]. The conformational change involves residues in ATP binding and phosphorylation domains, and it is transmitted to the extracytoplasmic surface with changes in binding affinity for cations and ouabain. In addition to bonds exposed to proteolysis, the transition involves tryptophans, sulfhydryl groups, prononizable groups and residues binding FITC and iodoacetamide fluorescein [103] (*see* previous reviews for details [68, 95]). This treatise will focus on attempts to identify residues in the amino acid sequences that undergo spatial rearrangements as part of E_1–E_2 transition and cation translocation.

A. Conformation-Dependent Proteolytic Cleavage of Na,K-ATPase

Definition of E_1 and E_2 conformations of α-subunit of Na,K-ATPase involves identification of cleavage

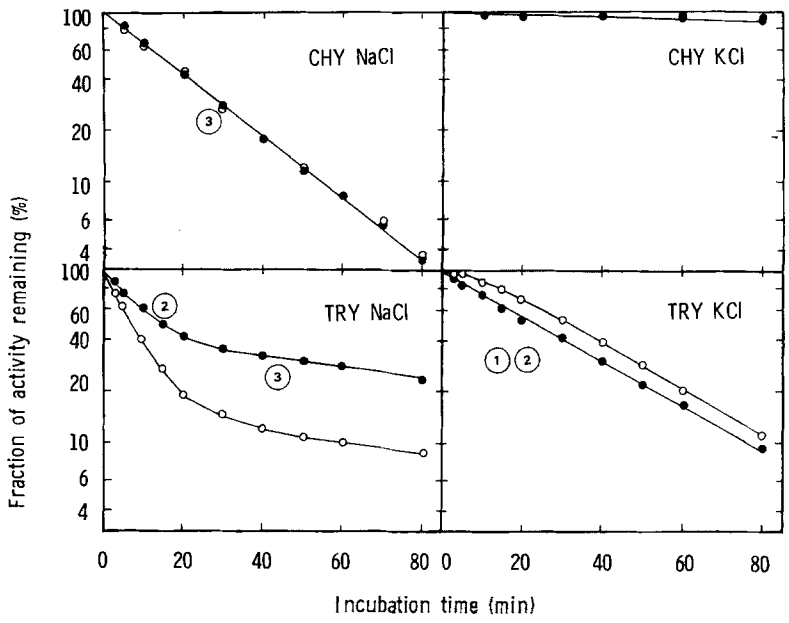

Fig. 6. Time course of inactivation of Na,K-ATPase (●) or K-phosphatase (○) by cleavage with chymotrypsin or trypsin in NaCl or KCl media. In NaCl, chymotrypsin (*CHY*) cleaves C_3 (Leu 266) and trypsin (*TRY*) cleaves T_2 (Arg 30) or T_3 (Arg 262) with biphasic inactivation pattern. In KCl, trypsin cleaves T_1 (Arg 438) and T_2 (Lys 30) in sequence. Redrawn from Refs. 93, 94, 100 and 101

points in the protein as well as association of cleavage with different rates of inactivation of Na,K-ATPase and K-phosphatase activities [93, 94]. In the E_1 form of Na,K-ATPase the cleavage patterns of the two serine proteases are clearly distinct. Chymotrypsin cleaves at Leu 266 (C_3), and both Na,K-ATPase and K-phosphatase are inactivated in a monoexponential pattern. Trypsin cleaves the E_1 form rapidly at Lys 30 (T_2) and more slowly at Arg 262 (T_3) to produce the characteristic biphasic pattern of inactivation shown in Fig. 6. Localization of these splits was determined by sequencing N-termini of fragments after isolation on high resolution gel filtration columns [100].

The E_2 form is not cleaved by chymotrypsin, but trypsin cleaves at Arg-438 (T_1) and subsequently at Lys-30 (T_2) and tryptic inactivation of E_2K or E_2P forms is linear and associated with cleavage at Arg-438 (T_1) [93, 100]. Inactivation of K-phosphatase is delayed because cleavage of T_1 and T_2 in sequence is required for inactivation of K-phosphatase activity [94]. A bond in the C-terminal half of α-subunit may be exposed in ouabain-bound complexes [25, 28].

Thus, transition from E_1 to E_2 consists of an integrated structural change involving protection of bond C_3 or T_3 in the second cytoplasmic domain and exposure of T_1 in the central domain, while position of T_2 in the N-terminus is altered relative to the central domain (T_1) so that cleavage of T_2 becomes secondary to cleavage of T_1 within the same α-subunit in the E_2-form.

B. Cleaved Derivatives of Na,K-ATPase

Selective cleavage of bonds in α-subunit of Na,K-ATPase is important for examining structure-function relationships for the protein. Table 2 shows the results of a series of experiments that allow distinction of direct modification of the function of ligand binding sites from effects on the conformational equilibria between E_1 and E_2 forms of the protein.

C. Cleavage of Bond 2 and Regulatory Function of N-Terminus

The N-terminus of the α-subunit is strongly hydrophilic with clusters of alternating positive and negative residues between residues 15 and 60. It is a flexible structure with a strong propensity for α-helix formation and several predicted turns, notably at residues 14–16, 35–26, 49–50 and 70–72. The removal of residues 1–30 by selective tryptic cleavage at Lys 30 (T_2) is possible because the rate of cleavage of this bond is up to 60-fold higher than the rate of tryptic cleavage at Arg-262 (T_3) in the second slow phase of inactivation. Removal of residues 1–

Table 2. Properties of unique cleaved derivatives of Na,K-ATPase

Enzymatic activity ligand binding or transport capacity	Cleavage		
	T_2 Lys-30	C_3 Leu-266	Control
Na,K-ATPase	40–50%	0%	100%
ATP-ADP exchange	150%	4–500%	100%
ATP binding			
Capacity	100%	100%	100%
Affinity (K_d μM)	—	.075	.045
Phosphorylation			
Capacity	100%	100%	100%
E_1P/E_2P ratio	55/45	100/0	14/84
Rb binding			
Capacity	100%	100%	100%
Affinity (K_d μM)	9–19	9–12	9–12
Rb-Rb exchange	ND	60–70%	100% (10–2 sec^{-1})
(P_i-ATP) Rb-Rb exchange	—	10%	100% (30–40 sec^{-1})
(ATP-ADP) Na-Na exchange	—	15%	100% (20–30 sec^{-1})
(ATP) Na,K transport	40–50%	17%	100% (491 sec^{-1})

Compiled from references 93–96, 101 and 102.

30 reduces Na,K-ATPase activity by 50–60% [94] with a parallel loss of Na,K-transport [108]. The loss of activity is explained by a poise of equilibria between cation bound (E_1Na–E_2K) and phosphoforms (E_1P–E_2P) in direction of E_1 forms [95]. These properties of the selectively cleaved derivative suggested that charged residues in the N-terminus engage in salt bridge formation as part of E_1–E_2 transition [100–102] and that this is important for control of the rate of active Na,K-transport by pumps containing the α isoform.

These data, in combination with the observation of substantial differences between amino acid sequences in the N-terminal region of the α, α+, and α-III isoforms [178] (*cf.* Fig. 3), suggest that the different properties of these isoforms may be explained by differences in rates of E_1–E_2 transitions. The first 30 residues of the α isoform has a high frequency of charges with eight lysines and two arginines. In the α+ isoform there are two negative and three positive charges fewer in this segment than in the α isoform suggesting that the strength of salt bridges formed with other segments may be weaker. The first 11 residues of α-III isoform are not homologous with the other isoforms, but all isoforms of α-subunit have a stretch of lysines around res. 30 [178]. Also the N-terminus of H,K-ATPase [180] possesses a lysine-rich sequence with strong homology with the α-subunit around T_2. Biphasic cleavage patterns resembling those in Na,K-ATPase have also been demonstrated in H,K-ATPase [167], but so far without identification of cleavage points.

The N-terminus in Ca-ATPase [19] has fewer charges and shows no homology with that of Na,K-ATPase and H,K-ATPase. There is no evidence for selective cleavage nor for a regulatory role of the region in control of E_1–E_2 and rate of transport of Ca^{2+}.

D. Effect of C_3 Cleavage on E_1P–E_2P Transition and Cation Exchange

The alternating exposure of T_1 (Arg-438) in the E_2-form and C_3 (Leu-266) or T_3 (Arg-262) in the E_1 form reflects that motion within the segment (M_r 18,170) between these bonds including the phosphorylated residue (Asp-369) is an important element in E_1–E_2 transition. This is illustrated by the widely different consequences of selective cleavage of C_3 and T_1 for E_1–E_2 transition and cation exchange.

C_3 cleavage is a selective and particularly efficient tool for examining structure-function relationships of the second cytoplasmic domain (Table 2). Binding affinities for ADP and ATP are reduced four- to fivefold while TNP-ATP and eosin bind with the same affinity as in native Na,K-ATPase [101, 102]. Nucleotide binding is not affected by K^+ or Rb^+ although cation sites are undamaged. Con-

versely the cleaved enzyme also binds ^{86}Rb with high affinity [101] and it occludes the cations, but cation binding and occlusion are unaffected by nucleotide.

Combination of C_3 and T_1 cleavages allowed comparison of the properties of four phosphopeptides, the intact α-subunit, and the 83-kDa, 47-kDa, and 18-kDa fragments [102]. Transfer of phosphate from ATP to the fragments remains sensitive to Na^+ but the 87-kDa and 18-kDa fragments are stabilized in the E_1P form. This is a specific effect of C_3 cleavage, because comparison with the properties of the 47-kDa fragment shows that after cleavage of T_1 alone, the 47-kDa fragment forms both E_1P and E_2P and the Na-Na and K-K exchange reactions are preserved. Stabilization of the protein in the E_1P form after C_3 cleavage allows demonstration of ^{22}Na occlusion [68] and the split abolishes the transient current associated with the translocation of Na^+ in the first turnover of the pump [9].

Transport studies in reconstituted vesicles show that C_3 cleavage blocks the relatively fast Na-Na or K-K exchange (20–40 sec^{-1}) and Na-K exchange (500 sec^{-1}), but the slow passive ouabain-sensitive Rb-Rb-exchange (1 sec^{-1}) and occlusion of K^+ or Na^+ are only partially affected. This is basis for the conclusion that C_3 cleavage interferes with coordination between structural changes of the phosphorylated segment and cation sites that may be formed by segments in the second cytoplasmic domain of the α-subunit [101, 102].

E. Identification of E_1–E_2 Forms in H,K-ATPase by Proteolysis

Tryptic cleavage of H,K-ATPase of gastric mucosa depends on conformation in patterns resembling those observed for Na,K-ATPase. In K^+ medium, in the E_2 form, cleavage is near the middle of the chain with appearance of fragments of 47 and 60 kDa. ATP and Mg^{2+} induces a biphasic time course of inactivation with appearance of a larger fragment with a mass of 78 kDa [167]. Fragments of 47 and 87 kDa are phosphorylated from ATP. Specific cleavage points have not been localized, but homologies with the α-subunit of Na,K-ATPase suggest that T_1 is found in H,K-ATPase at Lys-455. T_2 is probably at Lys-39 and the sequences around T_3 and C_3 in α-subunit of Na,K-ATPase are found at Lys-280 (T_3) and Leu-283 (C_3) in H,K-ATPase. These bonds have not been identified as cleavage points in H,K-ATPase, but cleavage here would result in fragment sizes of 84, 49, and 65 kDa, that agree well with the experimental observations [168].

F. Conformation-Dependent Cleavage in Ca-ATPase

Tryptic cleavage at T_1 (Arg 505) and T_2 (Arg 198) of Ca-ATPase produces three major fragments: A2 (res. 1–198), A1 (res. 199–505), and B (res. 306–1001) (128, 197). Cleavage at T_2 is conformation-dependent-like cleavage of T_3 and C_3 in the same domain of Na,K-ATPase [2, 3, 7, 89]. The ADP-sensitive phosphoenzyme, E_1P, exposes Arg-198 as does the unphosphorylated E_1 form. The bond is protected in both the ADP-insensitive phosphoenzyme, E_2P and in unphosphorylated E_2, stabilized with vanadate. This means that tryptic cleavage at Arg-198 defines the two major conformational classes of Ca-ATPase, irrespective of whether phosphate is bound or not [7]. The characteristic tryptic cleavage patterns of E_1 and E_2 states of Ca-ATPase are observed even after solubilization in monomeric form with octaethylene-glycol-monododecylether ($C_{12}E_8$) [5]. This shows that protection of the bond at Arg-198 in E_2 forms results directly from a change in folding of individual peptide chains rather than from a change of lipid-protein or protein-protein interaction. Further secondary splitting of the tryptic fragment A1 (res. 199–505) is also conformation dependent [88, 89].

G. Cleaved Derivatives of Ca-ATPase

Tryptic cleavage inhibits both ATP hydrolysis and Ca^{2+} transport, probably by interfering with transition from ADP-sensitive to ADP-insensitive phosphoenzyme [2, 88]. This effect is most pronounced after secondary cleavage of the A1 and A2 peptides to smaller fragments [88]. The functional disturbance may be due to loss of small peptide segments from the protein. Previously, an increased permeability of the membrane after tryptic digestion was interpreted as uncoupling of ATP hydrolysis from Ca transport [175]. This is basis for the use of the term "transduction domain" [19], but the permeability increase may be due to cleavage of other proteins in the sarcoplasmic reticulum membrane.

IX. Transposition of Mass Accompanying E_1–E_2 Transition

Altered degrees of immersion of protein into the hydrophobic environment of the membrane may be monitored by photoactivatable hydrophobic reagents [15]. Labeling of α-subunit of Na,K-ATPase [105] and Ca-ATPase [7] provide evidence that

movement of peptide segments between hydrophilic and hydrophobic environments may accompany E_1–E_2 transitions. The hydrophobic photoactivatable lable [^{125}J]-iodonaphtylazide [15] labels E_2 forms 10–25% more than E_1 forms of Na,K-ATPase [105]. A more detailed analysis shows that the hydrophobic photolabel [^{125}J]-trifluoromethyl-phenyldiazirine (TID) [23] may be used to determine relative accessibility of the peptide chain from the lipid phase in four different functional states of Ca-ATPase: E_1Ca_2, E_1PCa_2, E_2V and E_2 [7]. The phosphorylated E_1PCa_2 form was stabilized by use of CrATP as phosphorylating substrate, whereas the vanadate bound E_2V represented a stable E_2 state. In E_2 forms the degree of hydrophobic labeling was found to be 10–20% higher than in E_1 forms. The preferential hydrophobic labeling of E_2 forms was located on the C-terminal side of the conformational-sensitive tryptic split, with 70% higher labeling of the A1 fragment (res. 199–505) than of other segments of the Ca-ATPase protein. The A1 fragment also contains the phosphorylated aspartyl residue. Assuming that labeling with TID distributes evenly on peptide segments in contact with lipid [23] and that at least 200 amino acid residues are buried in the membrane in E_1 forms, it can be calculated that the different between hydrophobic labeling of E_1 and E_2 forms corresponds to movement of a minimum of 38 residues into the bilayer [7].

Examination of E_2 crystals of Ca-ATPase suggests a deeper immersion of the peptide chain in the bilayer relative to noncrystalline E_1 forms [31, 75]. Transposition of peptide mass from the cytoplasmic surface into the lipid phase during the functional cycle has also been inferred from time-resolved X-ray diffraction of oriented multilayers after synchronization of phosphorylation with caged ATP [16]. The observed change in X-ray diffraction pattern occurred with a rate constant which was higher than the assumed rate of E_1P–E_2P transition. Therefore it is not clear whether the movement detected in this way should be ascribed to phosphoenzyme isomerization or to formation of E_1P and concomitant Ca^{2+} occlusion.

A. Tryptophan Fluorescence

If E_1–E_2 transitions in both Na,K-ATPase and Ca-ATPase are accompanied by movement of peptide segments from cytoplasmic to hydrophobic environments if may appear surprising that changes in intensity of intrinsic fluorescence takes opposite directions in the two proteins. Tryptophan fluorescence is increased 2–3% by transition from E_1 to E_2 in Na,K-ATPase [109], while E_1–E_2 transition in Ca-ATPase causes a 4–5% reduction in fluorescence intensity [5, 46]. These qualitative differences in fluorescence of E_1 and E_2 forms of the two pump proteins may be understood in terms of different locations of the tryptophans in the protein structures. In Na,K-ATPase, only two of a total of 12 tryptophans in the α-subunit are located in predicted transmembrane segments, whereas all except two of the 13 tryptophans in Ca-ATPase are in the membrane region. Quenching analysis of Na,K-ATPase suggests that the tryptophan fluorescence changes are directly related to change of overall protein conformation [200]. For Ca-ATPase the increase of fluorescence accompanying Ca^{2+} binding may reflect local Ca-induced shielding from aqueous solvents of tryptophans that are located near the level of the phospholipid head groups [174]. Phosphoenzyme transition may be reflected by changes in position of Trp 552 in the nucleotide binding domain [27].

B. Secondary Structure Changes

Circular dichroism spectroscopy may detect changes in ratio between secondary structure elements, but even large shifts in position of α-helices and β-sheets relative to each other do not affect CD spectra. The question whether E_1–E_2 transitions are accompanied by changes in ratio among secondary structure elements raised some controversy. CD spectroscopy shows that Na,K-ATPase contains a roughly equal mixture of α-helical, β-sheet and random coil structures [74] and changes in CD spectra accompanying exchange of Na^+ for K^+ are interpreted to involve α-helix to β-helix to β-sheet transition of about 7% [74]. In contrast to this it was found by another group that addition of K^+ to a Tris-HCl medium did not cause changes in CD spectra [76]. In Ca-ATPase CD spectra remain unchanged during E_1–E_2 transition [35, 136].

X. Binding and Occlusion of Cations

A. Conformation of Occluded Complexes of Na,K-ATPase

Occluded cations are bound within the structure of the pump protein so that they are prevented from exchange with medium cations [157]. The presumptive occlusion cavity may be part of the transport pathway, because occlusion and release of cations

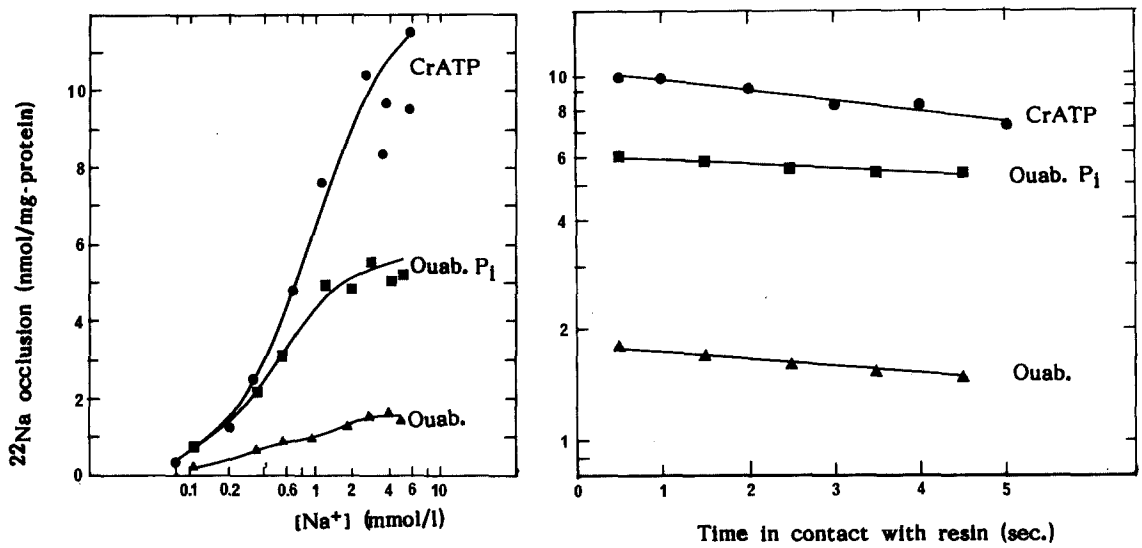

Fig. 7. ^{22}Na occlusion and deocclusion of membrane-bound Na,K-ATPase. Procedures were as described by Vilsen et al. [203]. *CrATP:* incubation with increasing concentrations of Na for 3 hr at 20°C with 0.5 mM CrATP, 1 mM $MgCl_2$, in 10 mM Tris, 0.1 mM EDTA, pH 7.5. *Ouabain:* incubation in the same buffer for 15 min at 20°C with 1 mM ouabain, 1 mM $MgCl_2$ with or without 1 mM P_i-Tris. For determination of the rate of deocclusion, the time spent in the Dowex was varied using a electrically operated automated syringe

from the cavity is governed by physiological ligands [107]. Recently, it was shown that the $\alpha\beta$-unit is the minimum functional unit for occlusion of ^{22}Na or ^{86}Rb in Na,K-ATPase [203]. This observation shows that the presumptive occlusion cavity is formed within the structure of an $\alpha\beta$-unit and that interaction between α-subunits is not required for occlusion.

Understanding the relationship between occlusion-deocclusion and E_1–E_2 transitions in the protein may be a key to solving the cation transport mechanism. It is therefore important to determine the protein conformations of the occluded complexes of Na,K-ATPase with Na^+ or Rb^+. It is generally accepted that Na^+ ions are occluded in E_1P[Na] phosphoforms and that Rb^+ (or K^+) are stabilized in an E_2[K] form, but as discussed below, there is also evidence for occlusion of Na^+ in E_2P forms and for occlusion of K^+ in E_1 forms of the protein.

Post et al. [157] operationally defined occlusion as the state of Rb^+ in Na,K-ATPase after dephosphorylation, but it is now clear that Rb^+/K^+ may enter and leave the occluded state at both membrane surfaces. Occlusion can be measured directly using Dowex columns [14, 69] or filters [60] for removing freely exchangeable cation. The capacity in purified Na,K-ATPase corresponds to two Rb^+ ions per $\alpha\beta$-unit both in the membranous and in the soluble state [203]. ATP and ADP act with low affinity (K_d 0.3–1 mM) to induce transition from $E_2(K2)_{occl}$ to E_1(K2)ATP and rapid release of both ions [68, 107, 109]. These are normal steps in the reaction cycle and represent a significant rate limitation in the pump cycle at low ATP [104]. Phosphorylation from P_i releases occluded Rb^+ or K^+ ions at the extracellular surface of the pump with rates of 5–15 sec^{-1} at 20°C. In presence of Na^+ both ions are rapidly released, but with K^+ in the medium there is slow release of one occluded ion. This lends support to a flickering gate hypothesis for deocclusion to the extracellular surface [61].

After cleavage of bond C_3 (Leu-266) with chymotrypsin [102] the E_1P form occludes Na^+ ions with a stoichiometry of 3Na/EP [68]. Lower capacities are seen after treatment with N-ethylmaleimide [68] or oligomycin [55]. With CrATP as phosphorylating substrate, values of ^{22}Na occlusion as high as 11 nmol/mg protein, were reached (Fig. 7) in selected purified preparations of Na,K-ATPase with 6 nmol EP/mg protein [203]. This yields a stoichiometry of 1.8 Na/EP, but appropriate extrapolation for unsaturation of binding sites corrects this value to 2.7 Na/EP. Phosphorylation from CrATP stabilizes a Na-occluded conformation. CrADP-E_1P[Na]. Examination of tryptic cleavage patterns of the CrADP-E_1P[Na] form, confirms that the α-subunit is cleaved according to the pattern that is characteristic for the E_1 form (*unpublished, cf.* 93). In Fig. 7, occlusion of Na^+ in CrADP-E_1P[Na] is compared with occlusion of Na^+ in complexes with ouabain (*cf.* 62). It is seen that the capacity for occlusion of Na^+ is low in presence of Mg^{2+} and ouabain, but that it is increased to 5–6 nmol/mg protein in pres-

ence of 1 mmol/liter phosphate without changing the apparent affinity for Na^+. Phosphorylation of the aspartyl residue may thus be necessary for occlusion or directly involved in coordinating the cation in the E_2 form. The capacity for Na^+ occlusion by the Ouab-E_2P[Na] complex is lower than that of the CrADP-E_1P[Na] complex. This may suggest that the transition from E_1P to E_2P involves the release of one of the occluded Na^+ ions as shown in Fig. 10(*a*).

Rb^+ (or K^+) ions are occluded in the E_2[Rb] form but there is also evidence for occlusion of Rb^+ in E_1 forms [101]. Formation of a ternary complex of Na,K-ATPase, K^+ and ATP is clearly demonstrated after cleavage by chymotrypsin or after blocking sulfhydryl groups. The chymotrypsin-cleaved enzyme occludes Rb^+ (or K^+) with high affinity in a process that is unaffected by ATP and without changes in fluorescence from intrinsic or extrinsic probes [101]. Na^+ and Rb^+ (or K^+) compete for occlusion in the chymotrypsin-cleaved E_1ATP form [101] and in complexes of Na,K-ATPase with ouabain and P_i [62]. This is in agreement with the notion that a single set of cation sites may bind and occlude either Na^+ or Rb^+ (or K^+). The evidence for formation of occluded complexes of the $\alpha\beta$-unit of Na,K-ATPase with Na^+ or Rb^+ (or K^+) in both E_1 and E_2 forms is basis for the reaction cycle and transport model in Fig. 10.

B. Occlusion of Ca^{2+}

Occlusion of Ca^{2+} is analogous to occlusion of Na^+ in E_1P of Na,K-ATPase. The occluded Ca^{2+} ions can be released on either side of the membrane, depending on whether the phosphoenzyme is permitted to undergo the transition to ADP-insensitive E_2P with luminally oriented Ca^{2+} sites or it is dephosphorylated by the backward reaction with ADP [45, 63, 190, 194]. A stable Ca^{2+}-occluded form can be obtained with CrATP as phosphorylating substrate [176, 202]. In this complex Ca^{2+} is occluded in a monomeric Ca-ATPase unit and the tryptic cleavage pattern is similar to the unphosphorylated E_1 form [7]. The structural rearrangements involved in occlusion may thus be of limited extent, possibly involving addition of a pair of coordinating groups and removal of the last few water molecules in the first coordination sphere of bound Ca^{2+}.

The demonstration of Ca-occluded E_1 forms of the protein [176, 202] suggests that phosphoryl transfer from ATP to the aspartyl residue accompanies occlusion of Ca^{2+}, while translocation and release of Ca^{2+} at the extra-cytoplasmic surface are coupled to the subsequent steps, E_1P–E_2P transition and dephosphorylation.

XI. Coupling of E_1–E_2 Transitions to Cation Transport

A. High and Low Energy Phosphate Forms, E_1P–E_2P

A fundamental property of E_1 and E_2 forms of both Na,K-ATPase and Ca-ATPase is their specific chemical reactivities. E_1 forms of both enzymes accept γ-phosphate from ATP, whereas E_2 forms react with P_i. E_1P forms are ADP sensitive, whereas E_2P forms do not transfer phosphate to ADP [39, 68]. The molecular basis for these distinctions has not been elucidated in detail, but proteolytic cleavage and hydrophobic labeling studies suggest that rearrangement of peptide structures formed from the segment connecting the second cytoplasmic domain with the phosphorylated aspartic acid residue may play an important role [102]. A separation of phosphate from the nucleotide site in E_2 forms was proposed as an interpretation of the effects of proteolytic cleavage of bonds 1 and 3 in the α-subunit of Na,K-ATPase on phosphorylation, dephosphorylation and cation exchange [102]. For Ca-ATPase a close relationship has been established between events in the catalytic site and reduction of Ca affinity (Fig. 8) [3, 39] leading to a form that releases Ca^{2+} at the luminal surface of the SR membrane.

Based on a series of studies of the effect of organic solvent on the reaction of Ca-ATPase with P_i and ATP synthesis, DeMeis proposed that a different solvent structure in the phosphate microenvironment in E_1 and E_2 forms the basis for existence of high and low energy forms of the aspartyl phosphate [39, 40, 154]. Acyl phosphates have relatively low free energy of hydrolysis when the activity of water is reduced, due to the change of solvation energy. The covalently bound phosphate may also reside in a hydrophobic environment in E_2P of Na,K-ATPase since increased partition of P_i into the site is observed in presence of organic solvent as shown in Fig. 9. It is seen that DMSO increases the affinity of Na,K-ATPase for inorganic phosphate in the same manner as in Ca-ATPase.

In line with this, fluorescence quenching [36, 47, 83], spin-label studies [32], and intramolecular cross-linking [164] suggest that the nucleotide site of Ca-ATPase undergoes rearrangements in relation to E_1P–E_2P transitions. The site has a lower accessibility to bulk solvent and a more hydrophobic character in E_2 forms, especially in E_2P relative to E_1 forms. Cross-linking experiments involving lysines near the active site in Ca-ATPase suggest that glutaraldehyde has restricted access to the active site in E_2P [164]. A tentative interpretation is that an interdomain movement closes the active site cleft.

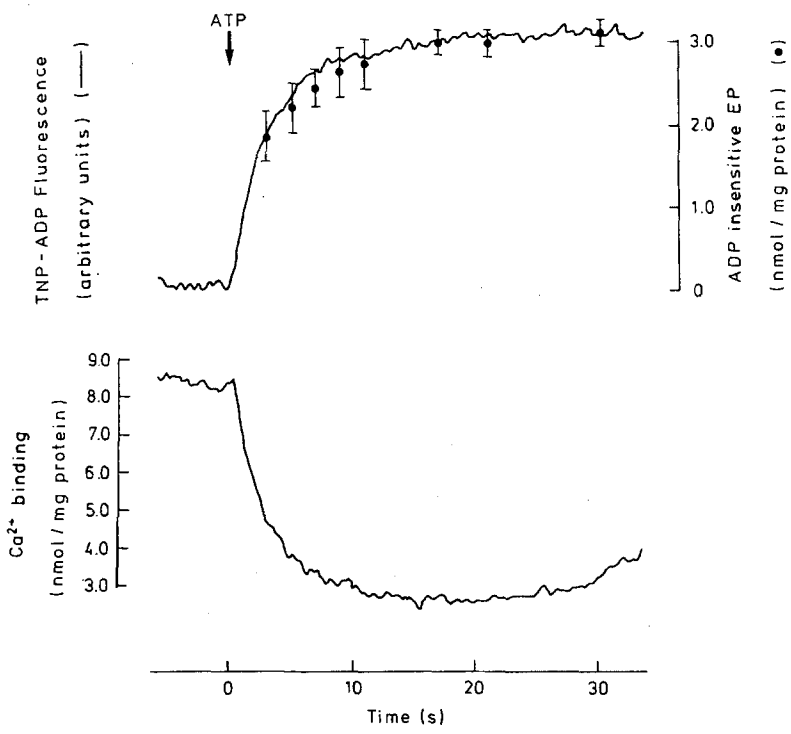

Fig. 8. Relationship between E_1P–E_2P transition and reduction of Ca^{2+} affinity in soluble monomeric Ca-ATPase. Upper panel shows appearance of ADP-insensitive E_2P and rise of fluorescence from bound TNP-ADP. Lower panel shows dissociation of Ca^{2+} due to E_1P–E_2P transition as measured with the indicator dye murexide. Modified from Ref. 3

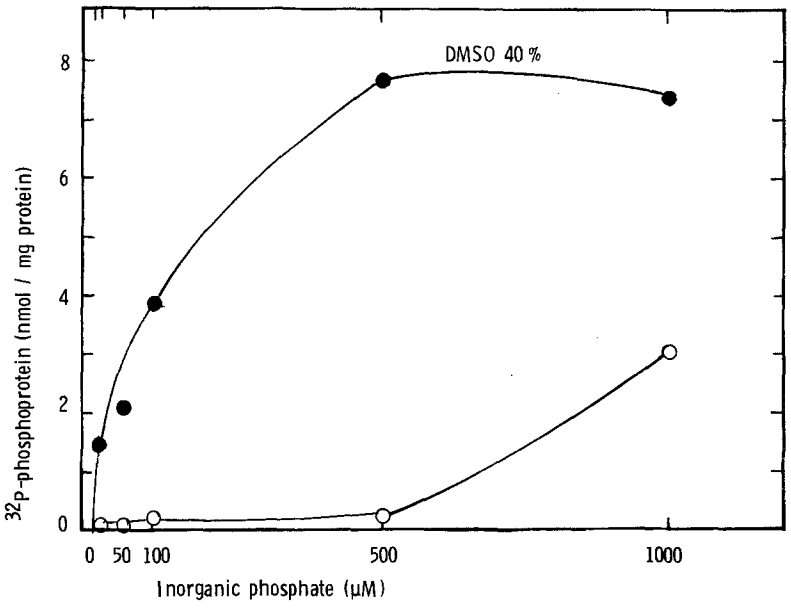

Fig. 9. Effect of DMSO on formation of acid-soluble phosphoenzyme from $^{32}P_i$ and purified Na,K-ATPase. It is seen that DMSO increases the apparent affinity of Na,K-ATPase for P_i from >1 mM to 120 μM. Conditions of experiment were similar to those used by DeMeis et al. for Ca-ATPase [40]

Closure of the open E_1P conformation during transition to E_2P may explain the restricted access of water and glutaraldehyde to the active site of the E_2P intermediate.

In the reaction scheme for Na,K-pumping in Fig. 10, the E_1–E_2 transitions constitute the cation translocation steps, Na extrusion involving the E_1P–E_2P transitions and K update the E_2K–E_1ATP transition. Na^+ and K^+ are transported in sequence, Na^+ first and then K^+ in a ping-pong, sequential reaction, but this model is challenged by some authors. In a recent review, Glynn [68] evaluates problems related to interpretation of kinetic studies with [γ^{32}P]-ATP and examines in detail the arguments for and against the competence of E_1P and E_2P in this transport cycle.

Recent developments have allowed more direct studies of the correlation between E_1–E_2 transitions

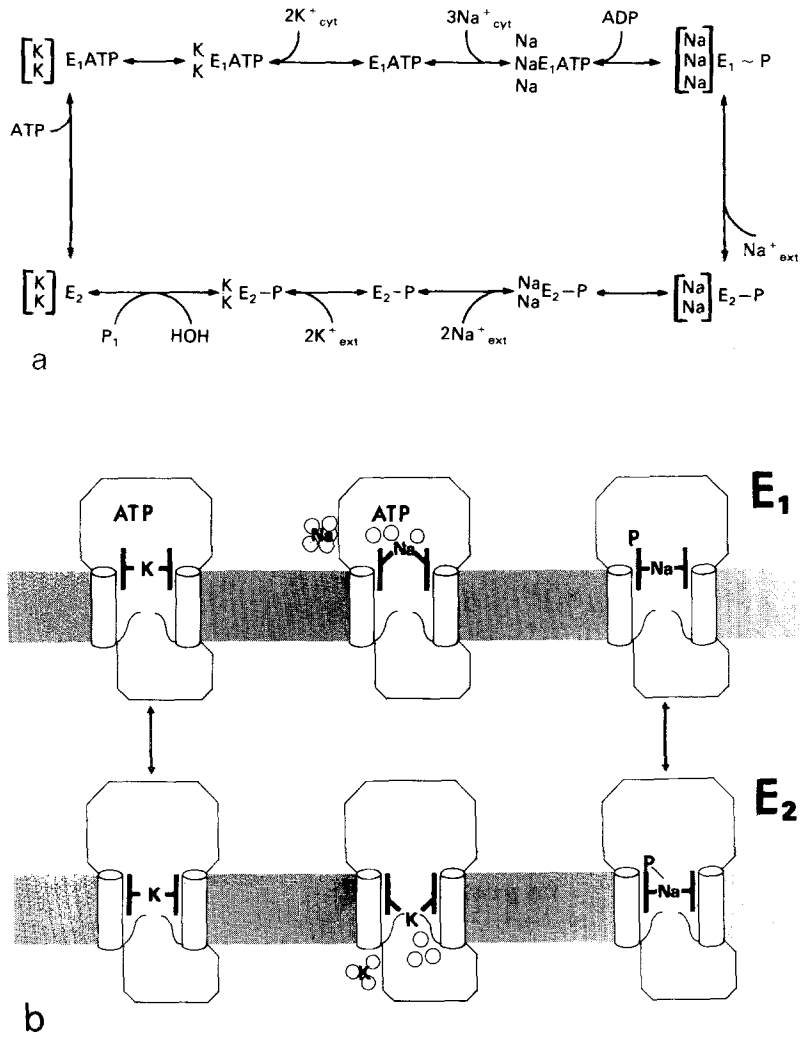

Fig. 10. (*a*) E_1–E_2 reaction cycle of the Na,K pump with four major occluded conformations and ping-pong sequential cation translocation. The phosphoforms occlude Na^+ and dephosphoforms occlude K^+ or Rb^+. Na^+ and K^+ without brackets are cations bound to an open form such that they can exchange with medium cation. [Na] or [K] within brackets are occluded and prevented from exchanging with medium cations. It is proposed that release of Na_{ext} accompanies transition from $E_1P[Na_3]$ to $E_2P[Na2]$ since capacity for occlusion of Na^+ in the ouabain-stabilized form is lower than after incubation with CrATP (Fig. 7). (*b*) A structure model for formation of cation pathway through the $\alpha\beta$-unit of Na,K-ATPase with reference to the reaction scheme in (*a*). The $\alpha\beta$-unit possesses cytoplasmic (α-subunit) and extracellular protrusions (β-subunit) and an intramembrane portion. The cylinders indicate a sheet of 8 + 1 transmembrane helices. Inside this sheet, a functional core organized in amphipatic helices or β-sheet structures forms the cation binding region. Motion of the cation coordinating groups constitutes an essential part of the E_1–E_2 transition. This transition effects transfer of occluded cations between a position near the intracellular aspect of the pump protein to a position near the extracellular mouth of the cation pathway. The E_1–E_2 transition involves transposition of mass from relatively hydrophilic to hydrophobic environments. This may be achieved by removing charges and exposing hydrophobic segments to the outer ring of hydrophobic transmembrane helices of the $\alpha\beta$-unit

and cation translocation. New techniques have been introduced for studying effects of membrane potential in reconstituted vesicles [162], presteady-state cation fluxes in vesicles [60, 106], and measurement of transient Na transport currents in planar lipid bilayers reconstituted with purified Na,K-ATPase [57, 134] and for voltage clamping in intact cells [41, 138]. Data from this work provide convincing evidence for correlation of ping-pong transport of Na^+ and K^+ with E_1–E_2 transitions in the protein.

B. E_1–E_2 Transitions in Vesicles Reconstituted with Purified Na,K-ATPase

The first problem in examining the relevance of E_1–E_2 transitions for active cation transport was to determine the sidedness of ligand effects on the conformation of the pump and the correlation between conformational changes and cation translocation. Tryptic digestion of Na,K pumps reconstituted with their cytoplasmic aspects facing outward gives biphasic or linear pattens of inactivation of Na,K transport that are similar to those for inactivatin of purified membrane-bound Na,K-ATPase [108]. These experiments show that K^+ and Na^+ ions stabilize E_2K or E_1Na, respectively, after combination with sites on the cytoplasmic surface.

Effects of electrical diffusion potentials on the individual conformational transitions can be examined after fluorescein labeling of reconstituted Na,K pumps with their cytoplasmic aspect facing outward. This permits examination of electrical diffusion potentials on the individual conformational transitions. It is observed that diffusion potentials do not affect rates of conformational transitions $E_1(K2)$–$E_2(K2)_{occl}$ or the cation titration of the equilibrium [162]. This observation suggests that the K-transport step itself does not move net charge across the membrane and that its rate would be independent of membrane potential. This has recently

been confirmed both in reconstituted vesicles [70] and in intact cells [41].

In contrast, the rate of $E_1P[3Na]_{occl}$–$E_2P[2Na]$ (Fig. 10) was accelerated about fourfold by a potential of 180 mV negative inside the vesicles [162]. This effect on the rate of the conformational transition agrees with effects of membrane potential on the rate of Na,K transport and the recent demonstration that the outward transport of Na^+ is electrogenic both in planar bilayers [57] and in heart cells [138].

C. Voltage-Sensitive Transport Steps and Presteady-State Fluxes

Membrane potential, negative inside accelerates the rate of ATP-dependent Na,K transport by pumps with their cytoplasmic aspects facing outward in the vesicle membrane. At saturating ATP concentration the E_1P–E_2P step is rate limiting and Na,K transport is accelerated about 30% by a potential of −180 mV [70]. This effect disappears at low ATP concentration, where the rate-limiting step is the $E_2[K2]$–$ATPE_1[K2]$ transition (Fig. 10). The interpretation is that there is one net positive charge in the transport domain when three Na^+ ions are bound, while there is no net mobile charge when two K^+ ions are bound. These observations are in agreement with studies on intact cells [41, 65].

Another important test of the E_1P–E_2P scheme and the coupling to ping-pong ion translocation is the separation of presteady-state Na^+ and K^+ fluxes in vesicles. Forbush [60] loaded right-side-out plasma membrane vesicles with caged ATP and initiated a single turnover of the pump with a flash of light. Karlish and Kaplan [106] measured ATP-dependent uptake of ^{22}Na in reconstituted vesicles at 0°C. Both experiments show an initial burst of ^{22}Na uptake reflecting transfer in the first turnover of the Na,K pump which is insensitive to K^+ at the extracellular surface. The time of appearance of the burst shows that Na^+ transport involves more steps than formation of E_1P and that Na^+ efflux is an early event in the pump cycle relative to K^+ influx.

D. Active Na,K-Transport by Purified Na,K-ATPase in Planar Lipid Bilayer

In a new reconstitution technique [57], membrane fragments containing purified Na,K-ATPase from kidney [102] are adsorbed to planar lipid bilayers. Light-induced conversion of caged ATP is used to study transient currents coupled to Na^+ ion transport in absence and presence of K^+ [57, 134]. The method allows differentiation between a K^+-independent, transient current and a $Na^+ + K^+$-dependent, stationary current reflecting the continuous operation of the Na,K pump. Selection of the change translocating step is possible since the transient current is selectively blocked by chymotryptic cleavage [9]. In view of the earlier demonstration that the cleavage of bond C_3 (Leu-267) of the α-subunit stabilizes Na,K-ATPase in the Na-occluded $E_1P[Na]$ form [102], the data show that reactions preceding $E_1P[Na3]$ are electrically silent. This identifies the E_1P–E_2P transition as the charge-translocating step. In the lipid bilayer, the Na^+ transport step coupled to E_1P–E_2P transition is electrogenic both in absence and presence of K^+ since Na^+ stimulates dephosphorylation at a low rate in absence of K^+ [57]. This is in agreement with recent observations on reconstituted vesicles [34]. Thus, measurement of transient Na^+ currents from transport by Na,K-ATPase in black lipid membranes shows that Na^+ is released as an early electrogenic event before K^+ is bound. The transient Na^+ current elicited upon lysis of caged ATP is in agreement with ping-pong transport of Na^+ first and then K^+ as shown in Fig. 10. These conclusions from work on the purified Na,K-ATPase in artificial bilayers are in perfect agreement with the detailed kinetic analysis of Na,K fluxes through the pump in red blood cells [167].

XII. Model for Occlusion and Translocation of Na^+ and K^+

The reaction cycle and transport models in Fig. 10 are based on evidence for the structure and function of cation pumps that was discussed in the preceding sections of this article. The functional unit is an $\alpha\beta$-unit (section VI), with cytoplasmic (section VII) and extracellular protrusions as revealed in three-dimensional models of crystals of Na,K-ATPase (section IV.B). In addition to the sheet of transmembrane helices predicted from analysis of hydroplots of the amino acid sequences (section IV.E), it is proposed that the pump has a core of intramembrane amphipathic helices or β-sheet structures (section IV.F), which participate in binding and translocation of cations. The demonstration of occluded E_1 and E_2 forms (section X) in combination with a single set of sites for binding of Na^+ or Rb^+ (section VII.C) forms the basis for proposing the moving pore model in which the steps of ion binding and occlusion are distinct from the E_1–E_2 transition. This model may be seen as alternative to a combination of gates or ionophores with a hydrated pore [*cf.* 19, 199].

The data in section X showed that Na^+ ions are

occluded in both the E_1P[Na3] and E_2P[Na2] forms and in Section XI the E_1P[Na3)–E_2P[Na2] transition is identified as the charge-translocating step. In the model in Fig. 10, dehydration of the cation and coordination in an occluded conformation are therefore considered to be principal conditions for translocation. Occlusion of Na^+ in the inward-facing E_1 configuration of the cation sites is assumed to occur at the level of transition between cytoplasmic and intramembrane portions of the protein. As part of the transposition of mass accompanying E_1–E_2 transition (section IX), the cation binding sites move, but only over a fraction of the transmembrane length of the protein. The outward-facing E_2 configuration of the cation sites is connected to the extracellular aqueous phases through an access mouth or channel.

In Fig. 10(*b*) the cation-binding sites consisting of electrophilic carbonyl groups are located in a cavity to accommodate the cations inside the protein. Transition from open to occluded forms of the inward (E_1)- or outward (E_2)-facing configurations involves only limited changes in conformation of carbonyl residues and a substitution of solvent molecules from the inner coordination sphere of the cation [101]. Dehydration of Na^+ takes place on the cytoplasmic surface and after coordination of the cation, the carbonyl groups rearrange from open to occluded form. An essential part of the E_1–E_2 transition is the movement of the residues possessing the coordinating carbonyl groups from the bottom of the cytoplasmic mouth to the bottom of the extracellular mouth of the cation pathway. At the extracellular mouth of the cation pathway the site shifts from closed to open configuration and Na^+ is rehydrated and released. The same set of coordinating groups, except phosphate, bind K^+ from the outside. The mouth of the cation pathway is similar to the mouth of the K channel which has the function of dehydrating K^+ before the ions can pass the narrow part of the channel [*cf.* 188].

Work in the authors' laboratories is supported by Danish Medical Research Council and Novo's Foundation.

References

1. Addison, R. 1986. *J. Biol. Chem.* **261:**14896–14901
2. Andersen, J.P., Jørgensen, P.L. 1985. *J. Membrane Biol.* **88:**187–198
3. Andersen, J.P., Jørgensen, P.L., Møller, J.V. 1985. *Proc. Natl. Acad. Sci. USA* **82:**4573–4577
4. Andersen, J.P., Møller, J.V. 1985. *Biochim. Biophys. Acta* **815:**9–15
5. Andersen, J.P., Møller, J.V., Jørgensen, P.L. 1982. *J. Biol. Chem.* **257:**8300–8307
6. Andersen, J.P., Vilsen, B. 1985. *FEBS Lett.* **189:**13–17
7. Andersen, J.P., Vilsen, B., Collins, J.H., Jørgensen, P.L. 1986. *J. Membrane Biol.* **93:**85–92
8. Andersen, J.P., Vilsen, B., Nielsen, H., Møller, J.V. 1986. *Biochemistry* **25:**6439–6447
9. Apell, H.J., Borlinghaus, R., Läuger, P. 1987. *J. Membrane Biol.* **97:**179–191
10. Aquila, H., Misra, D., Eulitz, M., Klingenberg, M. 1982. *Hoppe-Seyler's Z. Physiol. Chem.* **363:**345–349
11. Baba, A., Nakamura, T., Kawakita, M. 1986. *J. Biochem.* **100:**1137–1147
12. Baker, E.N., Hubbard, R.E. 1984. *Prog. Biophys. Mol. Biol.* **44:**97–197
13. Barrabin, H., Scofano, H.M., Inesi, G. 1984. *Biochemistry* **23:**1542–1548
14. Beaugé, J.A., Glynn, I.M. 1979. *Nature (London)* **280:**510–512
15. Bercovici, T., Gitler, C. 1978. *Biochemistry* **17:**1484–1489
16. Blasie, J.K., Herbette, L.G., Pascolini, D., Skita, V., Pierce, D.H., Scarpa, A. 1985. *Biophys. J.* **48:**9–18
17. Bowen, W.J., McDonough, A. 1987. *Am. J. Physiol.* **252:**C179–C189
18. Brandl, C.J., Deber, C.M. 1987. *Proc. Natl. Acad. Sci. USA* **83:**917–921
19. Brandl, C.J., Green, N.M., Korczak, B., MacLennan, D.H. 1986. *Cell* **44:**597–607
20. Brandl, C.J., Leon, S. de, Martin, D.R., MacLennan, D.H. 1987. *J. Biol. Chem.* **262:**3768–3774
21. Brotherus, J., Jost, P.C., Griffith, O.H., Keana, J.F.W., Hokin, L.E. 1980. *Proc. Natl. Acad. Sci. USA* **77:**272–276
22. Brown, T.A., Horowitz, B., Miller, R.P., McDonough, A.A., Farley, R.A. 1987. *Biochim. Biophys. Acta (in press)*
23. Brunner, J., Franzusoff, A.J., Lüscher B., Zugliani, C., Semenza, G. 1985. *Biochemistry* **24:**5422–5430
24. Castellani, L., Hardwicke, P.M.D., Vibert, P. 1985. *J. Mol. Biol.* **185:**579–594
25. Castro, J., Farley, R.A. 1979. *J. Biol. Chem.* **154:**2221–2228
26. Chadwick, C.C., Thomas, E.W. 1983. *Biochim. Biophys. Acta* **730:**201–206
27. Champeil, P., LeMaire, M., Moller, J.V., Riollet, S., Guillain, F., Green, N.M. 1986. *FEBS Lett.* **206:**93–98
28. Chin, G.J. 1985. *Biochemistry* **24:**5943–5947
29. Chin, G.J., Forgac, M. 1983. *Biochemistry* **22:**3405–3410
30. Chou, P.Y., Fassman, G.D. 1979. *Biophys. J.* **26:**367–384
31. Coan, C., Scales, D.J., Murphy, A.J. 1986. *J. Biol. Chem.* **261:**10394–10403
32. Coan, C., Verjovski-Almeida, S., Inesi, G. 1979. *J. Biol. Chem.* **254:**2968–2974
33. Cooper, J.B., Winter, C.G. 1980. *J. Supramol. Struct.* **3:**165–174
34. Cornelius, F., Skou, J.C. 1987. *In:* Na,K-ATPase. J.C. Skou, editor. A. Liss, New York (*in press*)
35. Csermely, P., Katopis, C., Wallace, B.A., Martonosi, A. 1987. *Biochem. J.* **241:**663–669
36. Davidson, G.A., Berman, M.C. 1987. *J. Biol. Chem.* **262:**7041–7046
37. Dayhoff, M.O., Schwarts, R.M., Orcutt, B.C. 1978. Atlas of Protein Sequence and Structure. Natl. Biomed. Res. Found. Washington, DC, pp. 345–363
38. Deisenhofer, J., Epp, O., Miki, K., Huber, R., Michel, H. 1985. *Nature (London)* **318:**618–624
39. De Meis, L. 1981. The Sarcoplasmic Reticulum. J. Wiley, New York

40. De Meis, L., Martins, O.B., Alves, E.W. 1980. *Biochemistry* **19:**4252–4261
41. De Weer, P., Gadsby, D.C., Rabowky, R.F. 1987. *J. Physiol. (London) (in press)*
42. Doolittle, R.F. 1985. *Trends Biochem. Sci.* **10:**233–237
43. Dorus, E., Hesse, J.E., Epstein, W. 1985. *In:* The Sodium Pump. I. Glynn and C. Ellory, editors. pp. 743–746. Company of Biologists, Cambridge
44. Doucet, A., Barlet-Bas, C. 1987. *In:* Na,K-ATPase. J.C. Skou, editor. A. Liss, New York *(in press)*
45. Dupont, Y. 1980. *Eur. J. Biochem.* **109:**231–238
46. Dupont, Y. 1982. *Biochim. Biophys. Acta* **688:**75–87
47. Dupont, Y., Pougeois, R. 1983. *FEBS Lett.* **156:**93–98
48. Dux, L., Papp, S., Martonosi, A. 1985. *J. Biol. Chem.* **260:**13454–13458
49. Dux, L., Pikula, S., Mullner, N., Martonosi, A. 1987. *J. Biol. Chem.* **262:**6439–6442
50. Dux, L., Taylor, K.A., Ting-Beall, H.P., Martonosi, A. 1985. *J. Biol. Chem.* **260:**11730–11743
51. Dzhandzhugazyan, K.N., Jørgensen, P.L. 1985. *Biochim. Biophys. Acta* **817:**165–173
52. Epstein, E. 1985. *Curr. Top. Membr. Transp.* **23:**153–175
53. Esmann, M. 1982. *Biochim. Biophys. Acta* **688:**251–259
54. Esmann, M., Marsh, D. 1985. *Biochemistry* **24:**3572–3578
55. Esmann, M., Skou, J.C. 1985. *Biochem. Biophys. Res. Commun.* **127:**857–863
56. Fambrough, M.D. 1987. *J. Biol. Chem. (in press)*
57. Fendler, K., Grell, E., Haubs, M., Bamberg, E. 1985. *EMBO J.* **4:**3079–3085
58. Filoteo, A.G., Gorski, J.P., Penniston, J.T. 1987. *J. Biol. Chem.* **262:**6526–6530
59. Fisher, J.A., Baxter-Lowe, L.A., Hokin, L.E. 1986. *J. Biol. Chem.* **261:**515–519
60. Forbush, B., III. 1984. *Anal. Biochem.* **140:**159–163
61. Forbush, B., III. 1987. *J. Biol. Chem.* **262:**11116–11127
62. Forbush, B., III. 1987. *In:* Na,K-ATPase. J.C. Skou, editor. A. Liss, New York *(in press)*
63. Froehlich, J.P., Heller, P.F. 1985. *Biochemistry* **24:**126–136
64. Fry, D.C., Kuby, S.A., Mildvan, A.S. 1985. *Biochemistry* **24:**4680–4694
65. Gadsby, D.C., Kimura, J., Noma, A. 1985. *Nature (London)* **315:**63–65
66. Geering, K., Meyer, D.I., Paccolat, M.P., Kraehenbühl, J.P., Rossier, B.C. 1985. *J. Biol. Chem.* **260:**5154–5160
67. Gilbert, W. 1985. *Science* **228:**823–824
68. Glynn, I.M. 1985. *In:* The Enzymes of Biological Membranes. A.N. Martonosi, editor. Vol. 3, pp. 35–114. Plenum, New York
69. Glynn, I.M., Howland, J.L., Richards, D.E. 1985. *J. Physiol. (London)* **368:**453–459
70. Goldshlegger, R., Karlish, S.J.D., Rephaeli, A., Stein, W.D. 1987. *J. Physiol. (London) (in press)*
71. Goormaghtigh, E., Chadwick, C., Scarborough, G.A. 1986. *J. Biol. Chem.* **261:**7466–7471
72. Gorga, F.R. 1985. *Biochemistry* **24:**6783–6788
73. Green, N.M., Allen, G., Hebdon, G.M. 1980. *Ann. N.Y. Acad. Sci.* **368:**149–158
74. Gresalfi, T.V., Wallace, B.A. 1984. *J. Biol. Chem.* **259:**2622–2628
75. Hasselbach, W., Medda, P., Migala, A., Agostini, B. 1983. *Z. Naturforsch.* **38c:**1015–1022
76. Hastings, D.F., Reynolds, J.A., Tanford, C. 1986. *Biochim. Biophys. Acta (in press)*
77. Hayashi, Y., Mimura, K., Matsui, H., Takagi, 1987. *In:* Na,K-ATPase. J.C. Skou, editor. A. Liss, New York *(in press)*
78. Hayashi, Y., Takagi, T., Kafzawa, S., Matsui, H. 1983. *Biochim. Biophys. Acta* **748:**153–167
79. Hebert, H., Jørgensen, P.L., Skriver, E., Maunsbach, A.B. 1982. *Biochim. Biophys. Acta* **689:**571–574
80. Hebert, H., Skriver, E., Maunsbach, A.B. 1985. *FEBS Lett.* **187:**182–187
81. Herrera, V.L.M., Emanuel, J.R., Rouz-Opazo, N., Levenson, R., Nadal Ginard, B. 1987. *J. Cell Biol.* **105:**1855–1865
82. Hesse, J.E., Wieczorek, L., Altendorf, K., Reicin, A.S., Dorus, E., Epstein, W. 1984. *Proc. Natl. Acad. Sci. USA* **81:**4746–4750
83. Highsmith, S. 1986. *Biochemistry* **25:**1049–1054
84. Highsmith, S., Cohen, J.A. 1987. *Biochemistry* **26:**154–161
85. Holland, E.C., Drickamer, K. 1986. *J. Biol. Chem.* **261:**1286–1292
86. Homareda, H., Kawakami, K., Nagano, K., Matsui, H. *In:* Na,K-ATPase. J.C. Skou, editor. A. Liss, New York *(in press)*
87. Hubert, J.J., Schenk, D.B., Skelly, H., Leffert, H.L. 1986. *Biochemistry* **25:**4156–4163
88. Imamura, Y., Kawakita, M. 1986. *J. Bichem.* **100:**133–141
89. Imamura, Y., Saito, K., Kawakita, M. 1984. *J. Biochem.* **95:**1305–1313
90. Jensen, J., Ottolenghi, P. 1983. *Biochim. Biophys. Acta* **731:**282–289
91. Jørgensen, A.O., Jones, L.R. 1986. *J. Biol. Chem.* **261:**3775–3781
92. Jørgensen, P.L. 1972. *J. Steroid Biochem.* **3:**181–191
93. Jørgensen, P.L. 1975. *Biochim. Biophys. Acta* **401:**399–415
94. Jørgensen, P.L. 1977. *Biochim. Biophys. Acta* **466:**97–108
95. Jørgensen, P.L. 1982. *Biochim. Biophys. Acta* **694:**27–68
96. Jørgensen, P.L. 1986. *Kidney Int.* **29:**10–20
97. Jørgensen, P.L. 1987. *In:* Na,K-ATPase. J.C. Skou, editor. A. Liss, New York *(in press)*
98. Jørgensen, P.L., Andersen, J.P. 1986. *Biochemistry* **25:**6439–6447
99. Jørgensen, P.L., Brunner, J. 1983. *Biochim. Biophys. Acta* **735:**291–296
100. Jørgensen, P.L., Collins, J.H. 1986. *Biochim. Biophys. Acta* **860:**570–576
101. Jørgensen, P.L., Petersen, J. 1985. *Biochim. Biophys. Acta* **821:**319–333
102. Jørgensen, P.L., Skriver, S., Hebert, H., Maunsbach, A.B. 1982. *Ann. N.Y. Acad. Sci.* **402:**203–219
103. Kapakos, J.G., Steinberg, M. 1986. *J. Biol. Chem.* **261:**2084–2089
104. Karlish, S.J.D. 1980. *J. Bioenerg. Biomembr.* **12:**111–136
105. Karlish, S.J.D., Jørgensen, P.L., Gitler, C., 1977. *Nature (London)* **269:**715–717
106. Karlish, S.J.D., Kaplan, J. 1985. *In:* The Sodium Pump. I. Glynn and C. Ellory, editors. pp. 501–506. Company of Biologists, Cambridge
107. Karlish, S.J.D., Lieb, W.R., Stein, W.D. 1982. *J. Physiol. (London)* **328:**333–350
108. Karlish, S.J.D., Pick, U. 1981. *J. Physiol. (London)* **312:**505–529
109. Karlish, S.J.D., Yates, D.W., Glynn, I.M. 1978. *Biochim. Biophys. Acta* **525:**252–264
110. Kawakami, K., Noguchi, S., Noda, M., Takahashi, H., Ohta, T., Kawamura, M., Nojima, H., Nagano, K., Hitose, T., Inayama, S., Hayashida, H., Miyata, T., Numa, S. 1985. *Nature (London)* **316:**733–736

111. Kawakami, K., Nojima, H., Ohta, T., Nagano, K. 1986. *Nucleic Acids Res.* **14**:2833–2844
112. Kawakami, K., Ohta, T., Nojima, H., Nagno, K. 1986. *J. Biochem.* **100**:389–397
113. Kawamura, M., Nagano, K. 1984. *Biochim. Biophys. Acta* **774**:188–192
114. Kolb, E., Hudson, P.J., Harris, J.I. 1980. *Eur. J. Biochem.* **108**:587–597
115. Kopito, R.R., Anderson, M., Lodish, H.F. 1987. *J. Biol. Chem.* **262**:8035–8040
116. Kyte, J. 1981. *Nature (London)* **292**:201–204
117. Kyte, J., Doolitle, R.D. 1984. *J. Mol. Biol.* **157**:105–132
118. Lee, J.A., Fortes, P.A.G. 1986. *Biochemistry* **25**:8133–8144
119. Leonards, K.S., Kutchai, H. 1985. *Biochemistry* **24**:4876–4884
120. Lytton, J. 1985. *J. Biol. Chem.* **260**:10075–10080
121. MacLennan, D.H., Brandl, C.J., Korczak, B., Green, N.M. 1985. *Nature (London)* **316**:696–700
122. MacLennan, D.H., Zubrzycka-Gaarn, E. Jørgensen, A.O. 1985. *Curr. Top. Membr. Transp.* **24**:337–368
123. McMenamin, M.A.S. 1987. *Sci. Am.* **256**:84–92
124. Maixent, J.M., Charlemagne, D., Chapelle, B., Lelievre, L.G. 1987. *J. Biol. Chem.* **262**:6842–6848
125. Makowsky, L.D., Caspar, L.D., Doodenough, D.A., Philips, W.C. 1982. *Biophys. J.* **37**:189–191
126. Martin, D.W. 1983. *Biochemistry* **22**:2276–2282
127. Martonosi, A. 1982. *Annu. Rev. Physiol.* **44**:337–355
128. Marver, D., Lear, S., Marver, L.T., Silva, P., Epstein, F.H. 1986. *J. Membrane Biol.* **94**:205–215
129. Michel, H., Weyer, K.A., Gruenberg, H., Dunger, I., Oesterhelt, D., Lottspeich, F. 1986. *EMBO J.* **5**:1149–1158
130. Modyanov, N.N., Arzamazova, N.M., Arystarkhova, E.A., Gevondyan, N.M., Ovchinnikov, Y.A. 1984. *Biol. Membr. (USSR)* **2**:844–848
131. Mohraz, M., Simpson, M.V., Smith, P.R. 1987. *J. Cell Biol.* **105**:1–8
132. Møller, J.V., Andersen, J.P., LeMaire, M. 1982. *Mol. Cell. Biochem.* **42**:83–107
133. Mostov, K.E., DeFoor, P., Fleischer, S., Blobel, G. 1981. *Nature (London)* **292**:87–88
134. Nagel, G., Fendler, F., Grell, E., Bamberg, E. 1987. *Biochim. Biophys. Acta (in press)*
135. Nakamoto, R.K., Inesi, G. 1984. *J. Biol. Chem.* **259**:2961–2970
136. Nakamoto, R.K., Inesi, G. 1986. *FEBS Lett.* **194**:258–262
137. Nakamura, J. 1987. *J. Biol. Chem.* **262**:14492–14497
138. Nakao, M., Gadsby, D.C. 1986. *Nature (London)* **323**:628–630
139. Nicholas, R.A. 1984. *Biochemistry* **23**:888–898
140. Noguchi, S., Noda, M., Takashi, H., Kawakami, K., Ohta, T., Nagano, K., Hirose, T., Inayama, S., Kawamura, M., Numa, S. 1986. *FEBS Lett.* **196**:315–319
141. Ohta, T., Nagano, K., Yoshida, M. 1986. *Proc. Natl. Acad. Sci. USA* **83**:2071–2075
142. Ohta, T., Yoshida, M., Nagano, K., Hirano, H., Kawamura, M. 1986. *FEBS Lett.* **204**:297–301
143. Ottolenghi, P., Nørby, J.G., Jensen, J. 1986. *Biochem. Biophys. Res. Commun.* **135**:1008–1014
144. Ovchinnikov, Y.A., Arsenyan, S.G., Broude, N.E., Petrukhin, K.E., Grishin, A.V., Aldanova, N.A., Arzamazova, N.M., Arystarkhova, E.A., Melkov, A.M., Smirnov, Y.V., Guryev, S.O., Monastyrskaya, G.S., Modyanov, N.N. 1985. *Proc. Acad. Sci. USSR* **285**:1490–1495
145. Ovchinnikov, Y.A., Demin, V.V., Barnakov, A.N., Kuzin, A.P., Lunv, A.V., Modyanov, N.N., Dzhandzhugazyan, K.N. 1985. *FEBS Lett.* **190**:73–76
146. Ovchinnikov, Y.A., Demin, V.V., Modyanov, N.N., Dzhandzhugazyan, K.N. 1986. *Biol. Membr.* **5**:357–363
147. Ovchinnimov, Y.A., Dzhandzugazyan, K.N., Lutsenko, S.V., Mustayev, A.A., Modyanov, N.N. 1987. *FEBS Lett.* **217**:111–116
148. Ovchinnikov, Y.A., Modyanov, N.N., Broude, N.E., Petrukhin, K.E., Grishin, A.V., Arzamazova, N.M., Aldanova, N.A., Monastyrskaya, G.S., Sverdlov, E.D. 1986. *FEBS Lett.* **201**:237–245
149. Ovchinnikov, Y.A., Monastyrskaya, G.S., Broude, N.E., Allikmets, R.L., Ushkaryov, Y.A., Melkov, A.M., Smirnov, Y.V., Malyshev, I.V., Dulubova, I.E., Petrukhin, K.E., Gryshin, A.V. Sverdlov, V.E., Kiyatkin, N.I., Kostina, M.B., Modyanov, N.N., Sverdlov, E.D. 1987. *FEBS Lett.* **213**:73–80
150. Padgett, R.A., Grabowski, P.J., Konarska, M.M., Seiler, S., Sharp, P.A. *1986. Annu. Rev. Biochem.* **55**:1119–1150
151. Paul, C., Rosenbusch, J.P. 1985. *EMBO J.* **4**:1593–1597
152. Paul, D.L. 1986. *J. Cell. Biol.* **103**:123–134
153. Pedemonte, C.H., Kaplan, J.H. 1986. *J. Biol. Chem.* **261**:3632–3639
154. Pedersen, P.L., Carafoli, E. 1987. *Trends Biochem. Sci.* **12**:186–189
155. Pick, U., Karlish, S.J.D. 1982. *J. Biol. Chem.* **257**:6120–6126
156. Pick, U., Weiss, M. 1985. *Eur. J. Biochem.* **152**:83–89
157. Post, R.L., Hegyvary, C., Kume, S. 1972. *J. Biol. Chem.* **247**:6530–6540
158. Pressley, T.A., Edelman, I.S. 1986. *J. Biol. Chem.* **261**:9779–9786
159. Rabon, E., Wilke, M., Sachs, G., Zampighi, G. 1986. *J. Biol. Chem.* **261**:1434–1439
160. Rayson, B.M., Gupta, R.K. 1985. *J. Biol. Chem.* **260**:12740–12743
161. Reithmaier, R.A.F., MacLennan, D.H. 1981. *J. Biol. Chem.* **256**:5957–5960
162. Rephaeli, A., Richards, D.E., Karlish, S.J.D. 1986. *J. Biol. Chem.* **261**:6248–6254
163. Rephaeli, A., Richards, D.E., Karlish, S.J.D. 1986. *J. Biol. Chem.* **261**:12437–12440
164. Ross, D.C., McIntosh, D.B. 1987. *J. Biol. Chem.* **262**:2042–2049
165. Rossmann, M.G., Liljas, A., Branden, C.I. Babaszak, L.J. 1975. *In:* The Proteins. P.D. Boyer, editor. Vol. 11a, p. 62–103. Academic, New York
166. Sabatini, D.D., Kreibich, G., Morimoto, T., Adesnik, M. 1982. *J. Cell Biol.* **92**:1–22
167. Saccomani, G., Dailey, D.W., Sachs, G. 1979. *J. Biol. Chem.* **254**:2821–2827
168. Sachs, J.R. 1986. *J. Physiol. (London)* **381**:149–168
169. Schmitt, C.A., McDonough, A.A. 1986. *J. Biol. Chem.* **261**:10439–10444
170. Schneider, J.W., Mercer, R.W., Benz, E.J. 1987. *In:* Na,K-ATPase, J.C. Skou, editor. A. Liss, New York (*in press*)
171. Schnellenberg, G.D., Pech, I.V., Stahl, W.L. 1981. *Biochim. Biophys. Acta* **649**:691–700
172. Scott, T.L. 1984. *J. Biol. Chem.* **259**:4035–4037
173. Scott, T.L. 1985. *J. Biol. Chem.* **260**:14421–14423
174. Scott, T.L. 1986. *Biophys. J.* **49**:234a
175. Scott, T.L., Shamoo, A.E. 1982. *J. Membrane Biol.* **64**:137–144

176. Serpersu, E.H., Kirch, U., Schoner, W. 1982. *Eur. J. Biochem.* **122:**347–354
177. Serrano, R., Kielland-Brandt, M.C., Fink, G.R. 1986. *Nature (London)* **319:**689–693
178. Shull, G.E., Greeb, J., Lingrel, J.b. 1986. *Biochemistry* **25:**8125–8132
179. Shull, G.E., Lane, L.K., Lingrel, J.B. 1986. *Nature (London)* **321:**429–431
180. Shull, G.E., Lingrel, J.B. 1986. *J. Biol. Chem.* **261:**16788–16791
181. Shull, G.E., Schwartz, A., Lingrel, J.B. 1985. *Nature (London)* **316:**691–698
182. Shull, M.M., Lingrel, J.B. 1987. *Proc. Natl. Acad. Sci. USA* **84:**4039–4043
183. Skriver, E. Maunsbach, A.B., Jørgensen, P.L. *FEBS Lett.* **131:**219–222
184. Skulachev, V.P. 1985. *Eur. J. Biochem.* **151:**199–208
185. Solioz, M. Mathews, S. Furst, P. 1987. *J. Biol. Chem.* **262:**7458–7462
186. Specht, S., Sweadner, K. 1984. *Proc. Natl. Acad. Sci. USA* **81:**1234–1238
187. Squier, T.C., Bigelow, D.J., Ancos, J.G. de, Inesi, G. 1987. *J. Biol. Chem.* **262:**4748–4754
188. Stein, W.D. 1986. Transport and Diffusion Across Cell Membranes. Academic, New York
189. Stephens, E.M., Grisham, C.M. 1979. *Biochemistry* **18:**4876–4885
190. Sumida, M., Tonomura, Y. 1974. *J. Biochem.* **75:**283–297
191. Sweadner, K.J. 1979. *J. Biol. Chem.* **254:**6060–6067
192. Sweadner, K.J. 1985. *J. Biol. Chem.* **260:**11508–11513
193. Tada, M., Katz, A.M. 1982. *Annu. Rev. Physiol.* **44:**401–423
194. Takisawa, H., Makinose, M. 1983. *J. Biol. Chem.* **258:**2986–2992
195. Tamkun, M.M., Fambrough, D.M. 1986. *J. Biol. Chem.* **261:**1009–1019
196. Tanford, C. 1982. *Proc. Natl. Acad. Sci. USA* **79:**2881–2884
197. Taylor, K.A., Dux, L., Martonosi, A. 1986. *J. Mol. Biol.* **187:**417–427
198. Thorley-Lawson, D.A., Green, N.M. 1977. *Biochem. J.* **167:**739–748
199. Tonomura, Y. 1986. Energy Transducing ATPases-Structure and Kinetics. Cambridge University Press, London
200. Tyson, P., Steinberg, M. 1987. *J. Biol. Chem.* **262:**4644–4648
201. Verrey, F., Schaerer, E., Moerkler, P., Paccolat, M.P., Gehring, K., Kraehenbuhl, J.P., Rossier, B. 1987. *J. Cell Biol.* **104:**1231–1237
202. Vilsen, B., Andersen, J.P., 1986. *Biochim. Biophys. Acta* **855:**429–431
203. Vilsen, B., Andersen, J.P., Petersen, J., Jørgensen, P.L. 1987. *J. Biol. Chem.* **262:**10511–10517
204. Vyas, N.K., Vyas, M.N., Quiocho, F.A. 1987. *Nature (London)* **327:**635–638
205. Walker, J.E., Saraste, M., Runswick, M.J., Gay, N.J. 1982. *EMBO J.* **1:**945–951
206. Wallace, B., Cascio, M., Mielke, D.L. 1986. *Proc. Natl. Acad. Sci. USA* **83:**9423–9427
207. Wolitzky, B.A., Fambrough, D.M. 1986. *J. Biol. Chem.* **261:**9990–9999
208. Yamanaka, N., Deamer, W. 1976. *Biochim. Biophys. Acta* **426:**132–147
209. Yamashita, T., Kawakita, M. 1987. *J. Biochem.* **101:**377–385
210. Young, R.M., Lingrel, J.B. 1987. *J. Biol. Chem. (in press)*
211. Young, R.M., Shull, G.E., Lingrell, J.B. 1987. *J. Biol. Chem. (in press)*
212. Zamphigi, G., Kyte, J., Freytag, W. 1984. *J. Cell. Biol.* **98:**1851–1864
213. Zibirre, R., Hippler-Feldtmann, G., Kühne, J., Poronnik, P., Warnecke, G., Koch, G. 1987. *J. Biol. Chem.* **262:**4349–4354
214. Zubrycka-Gaarn, E., MacDonald, G., Phillips, L., Jorgensen, A.O., MacLennan, D.H. 1984. *J. Bioenerg. Biomembr.* **16:**441–464

Received 7 January 1988